TOWARDS IMPROVING P300-BASED BRAIN-COMPUTER INTERFACES: FROM DESKTOP TO MOBILE

A Dissertation
Submitted to the Graduate Faculty
of the
North Dakota State University
of Agriculture and Applied Science

By

Qasem Turki Obeidat

In Partial Fulfillment of the Requirements
for the Degree of
DOCTOR OF PHILOSOPHY

Major Department:
Computer Science

March 2014

Fargo, North Dakota

North Dakota State University
Graduate School

Title

TOWARDS IMPROVING P300-BASED BRAIN-COMPUTER INTERFACES: FROM DESKTOP TO MOBILE

By

Qasem Turki Obeidat

The Supervisory Committee certifies that this ***disquisition*** complies with North Dakota State University's regulations and meets the accepted standards for the degree of

DOCTOR OF PHILOSOPHY

SUPERVISORY COMMITTEE:

Dr. Jun Kong
Chair

Dr. Simone Ludwig

Dr. Rui Dai

Dr. Jerry Gao

Approved:

04/10/2014
Date

Dr. Brian Slator
Department Chair

ABSTRACT

A brain-computer interface (BCI) enables a paralyzed user to interact with an external device through brain signals. A BCI measures identifies patterns within these measured signals, translating such patterns into commands. The P300 is a pattern of a scalp potentials elicited by a luminance increment of an attended target rather than a non-target character of an alphanumeric matrix. The Row-Column Paradigm (RCP) can utilize responses to series of illuminations of matrix target and non-target characters to spell out alphanumeric strings of P300-eliciting target characters, yet this popular RCP speller faces three challenges. The *adjacent problem* concerns the proximity of neighboring characters, the *crowding problem* concerns their number. Both adjacent and crowding problems concern how these factors impede BCI performance. The *fatigue problem* concerns how RCP use is tiring. This dissertation addressed these challenges for both desktop and mobile platforms.

A new P300 speller interface, the Zigzag Paradigm (ZP), reduced the adjacent problem by increasing the distance between adjacent characters, as well as the crowding problem, by reducing the number neighboring characters. In desktop study, the classification accuracy was significantly improved 91% with the ZP VS 80.6% with the RCP.

Since the ZP is not suitable for mobile P300 spellers with a small screen size, a new P300 speller interface was developed in this study, the Edges Paradigm (EP). The EP reduced the adjacent and crowding problems by adding flashing squares located

upon the outer edges of the character matrix in the EP. The classification accuracy of the EP (i.e., 93.3%) was significantly higher than the RCP (i.e., 82.1%). We further compared three speller paradigms (i.e., RCP, ZP, and EP), and the result indicated that the EP produced the highest accuracy and caused less fatigue. Later, the EP is implemented in a simulator of a Samsung galaxy smart phone on the Microsoft Surface Pro 2. The mobile EP was compared with the RCP under the mobility situation when a user is moving on a wheelchair. The results showed that the EP significantly improved the online classification accuracy and user experience over the RCP.

DEDICATION

For my parents, Turki & Malaka,

my wonderful wife, Ola,

and my kids, Turki & Judy.

ACKNOWLEDGMENTS

I sincerely thank Allah the Most Beneficent, the Most Merciful, for countless bounties he has given me during my life, which guide and help me to complete one of the most exciting journeys in my life.

I am truly thankful for my Ph.D. advisor Dr. Jun Kong, a formidable mentor for me, for his priceless advice, guidance, assistance, support, encouragement and patience from the first day of my study. I remember that during my first meeting with Jun at his office, I felt comfortable, confident, and optimistic that I want to work with this special person based of his insightful discussions about the research.

I would also like to thank my dissertation committee members, Dr. Simone Ludwig, Dr. Rui (April) Dai, and Dr. Zhili (Jerry) Gao for their invaluable suggestions, support, and comments.

In addition, I would like to thank my friends and colleagues in North Dakota State University for their help and encouragement throughout to solve all my personal and academic challenges I faced during my journey.

My special thanks goes out to my special friend Dr. Tom Campbell, cognitive neuroscientist from University of Helsinki. I would never have been able to finish my dissertation without his endless support, guidance, help, motivation, and participation in each single point in this work. I truly thank Tom for everything he has done for me.

My thesis completion could not have been accomplished without my beloved parents, Turki and Malaka, pray and love. They were always supporting and encouraging me with their experience and best wishes through my entire life. I cannot forget to heartily thank my wife, Ola, and my kids, Turki and Judy, for allowing me time away from them to research.

TABLE OF CONTENTS

LIST OF TABLES

LIST OF FIGURES

CHAPTER 1. INTRODUCTION

This Information Age, an era of paperless organizations, remote work, electronic mail, electronic journals, electronic timetables, and web mapping services, has brought us more independence - an independence from which individuals with severe neuromuscular disease could, in principle, benefit to lead productive fulfilling lives [80]. Research into Brain-Computer Interfaces (BCIs) has, over the last two decades, emerged as a burgeoning field, offering modest improvements in quality of life to paralyzed individuals with minimal voluntary muscular control [86]. These individuals affected by a severe neuromuscular disease (e.g., Amyotrophic Lateral Sclerosis (ALS), spinal cord injury, brainstem stroke, or muscular dystrophies [96] have remained unable in any conventional manner to directly access many forms of information and communication technology such as computers and mobile phones, which are increasingly becoming more essential to our everyday activities. As a substitute for orthodox communication channels (e.g., a keyboard, mouse, touch screen, or voice recognition), BCI has set up a direct communication channel between the user's brain and a computer, such that the disabled user can control an external device or interact with application software through brain signals.

The BCI research studies indicate there is a bright future for individuals with minimal voluntary muscular control, as these individuals promise to offer an opportunity to increase their confidence, make their life enjoyable and easier, and enable them to depend on themselves interacting with external devices and new technologies. BCI technology, especially a P300-based BCI, has been applied successfully in a lab in many different domains, and allowed disabled people limited communication with other people, applications, and with external devices, including a motorized wheelchair [48], the control of prosthetic devices [44], a smart home [40], a brain-controlled internet browser [69, 99], a mobile address-book dialling application [16],

and a spelling system [25].

The P300 BCI applications have utilized a high amplitude component of the brain's electrical response to visual stimulation [87], variously known as the P300 or P3b, as is derived from Electroencephalography (EEG) measured via electrodes attached to the user's scalp and elicited during the processing of an attended target yet not by a to-be-ignored non-target stimulus [75]. Solutions to the electromagnetic inverse problem [42] have indicated that this scalp-measured P300 component is a consequence of neurocognitive processes [22, 54, 75, 76] affecting multiple source generators in the temporal and parietal lobes of the cerebral cortex of neurologically normal individuals [11, 67, 79].

Of such BCIs, the P300-based BCI speller, first introduced by Farwell and Donchin [25], has become the most extensively investigated approach. This speller is used to select one target object from multiple non-target objects, and has employed the oddball paradigm containing a rare target object stimulus interspersed among frequent non-target objects. The long-lasting P300 is characterized by a high-amplitude positive peak component of the Event-Related Potential (ERP); a component that is maximal over the user's scalp with a peak latency of around 300 ms after the stimulus onset.

Specifically, Farwell and Donchin's speller consisted of a 6-by-6 matrix of 36 alphanumeric characters displayed on a screen in front of a user, which has been termed the matrix speller or, more commonly, the row-column paradigm (RCP) [25], as shown in Figure 1. The rows and columns are flashed alternately in a randomized order, while the user's attention is focused upon the target character to silently count how many times the target character is flashed. Once the row or column containing a target character is flashed, a rare event, the P300 component is elicited. A classification algorithm is then applied to the collected EEG data to determine

the row and column that *elicited* the largest P300 amplitude, after which the target is identified as the intersection of that row and that column. Though RCP has been widely used, the paradigm has faced several challenges, namely the *adjacency*, *crowding*, and *fatigue* problems. These problems affect the performance and user experience of the RCP.

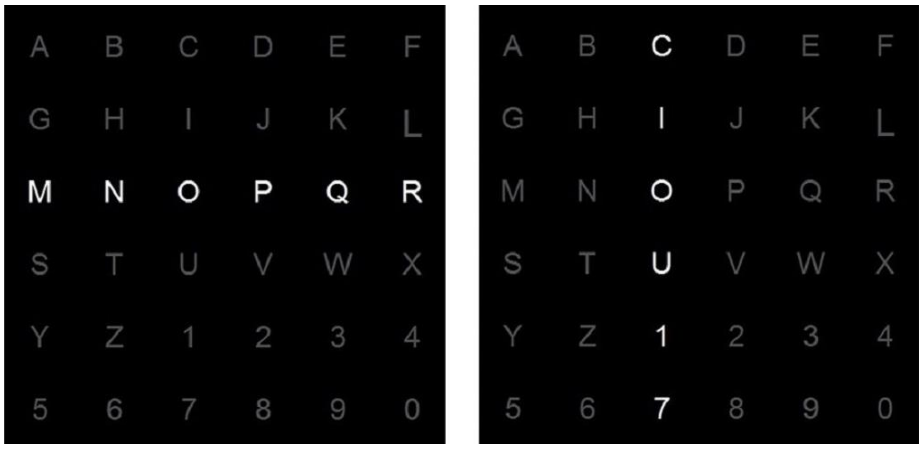

Figure 1. Classical row-column paradigm (RCP).

1.1. Motivation

The richness of the inner life of some individuals with minimal muscular control, undistracted by the pedestrian activities of the able-bodied, has brought new scientific insights – such as those popularized in *A Brief History of Time* [43] – together with some phenomenal literary contributions: After a cortico-subcortical stroke [9] afflicted Jean-Dominique Bauby with locked-in syndrome [23], such that the only way left to communicate was via blinks of his left eye, the former editor of *Elle* composed his memoirs, *The Diving Bell and the Butterfly* [5]. He recounts that while his whole body was held prisoner in a giant invisible diving-bell, he found freedom in his memories and imagination, which soared as a butterfly over the mountains – notions he communicated in the blink of an eye. Bauby wrote via partner-assisted scanning which relies upon another who presents a series of items, such as the alphabet; that

person decodes responses, such as a blink to select an item, a specific letter.

The main motivation of this research is to offer some advantages for people, especially the paralyzed people, like Bauby, and improve their quality of life even if it is limited. To achieve this research motivation, new P300 BCIs are described with new visual interfaces and a stimulus technique. These new P300 BCIs can reduce the scope for error caused when a user misses a target selection from the visual interface of the RCP by reducing the effect of the RCP problems.

According to a U.N. report in 2013, 85% of people on the planet, seven billion people worldwide, own a mobile phone [70]. A mobile phone is progressively becoming an essential wireless communication device in modern life; specifications developing rapidly, containing many advanced features and applications. In addition, there are some wireless EEG devices used in BCI research and commercially-available, such as the Emotiv EEG headset. Motivated by the aforementioned wireless devices available with high efficiency, to some extent, this research proposes to apply a new P300 BCI on a mobile phone, and offer a portable mobile P300 BCI. This work can enable paralyzed users to benefit from the fast developments in the mobile computing.

1.2. Problem Statement and Objectives

Though the original RCP speller provides a solution for disabled people to interact with a computer system, this speller still faces several problems, and this research focuses on the following problems:

1. The adjacent problem: the small distance between two adjacent characters has been identified as the major factor affecting accuracy [27, 72, 90]. Flashes are assumed to distract the user more when a character closer to the target character is flashed and the user is attempting to focus upon that target character. Accordingly, P300 elicitation is affected by evoking a P300 component in response to the non-target character flashes rather than to the target character flash, and

consequently trigger a false stimulus, which leads to a false recognition that is termed an adjacent error.

2. The crowding problem: crowding refers to the phenomenon that the identification of objects is hampered if they are surrounded by identical objects [12]. This crowding problem becomes more severe when the number of surrounding non-target characters increases [29]. Consequently, the visual discrimination of the target character becomes more difficult [30].

3. The fatigue problem: after using the RCP for a while, the subject feels tired, drowsy or loses his or her concentration, and this feeling affects the pattern recognition of brain activities that make the target character identification very difficult.

The main objective of this study was to develop new visual interfaces and flashing techniques for the P300 BCI from desktop to mobile, which is intended to address the adjacency, crowding and fatigue problems of the classical row column paradigm (RCP). This main objective is discussed into two points as follow:

1. In order to address the aforementioned RCP problems, we redesign the P300 spellers from the perspective of the visual layout and flashing technique. Those novel designs may reduce potential errors by increasing the distance between characters and reducing the number of other characters surrounding a character.

2. Little work has been conducted on developing BCIs on mobile devices. This dissertation intends to integrate BCIs with smart phones so that disabled users can also benefit from the fast development of mobile techniques. However, it is challenging to design mobile BCIs due to the small screen and complex interaction environments (e.g., noise or mobility).

1.3. Contributions

This dissertation makes three contributions:

1. The design of the ZP as an alternative P300-based BCI paradigm to the RCP. The ZP increases the distance between the adjacent characters and reduces the number of characters surrounding a character. In the ZP interface every second row of the 6-by-6 character matrix is offset to the right by $d/2$ cm, where d cm is the horizontal distance between two adjacent characters. Accordingly, an empirical investigation was conducted to evaluate the predicted improvements in performance and user experience with ZP. This investigation revealed that the ZP significantly improved the online performance accuracy and the user experience as well relative to the RCP.

2. The design of a new novel visual interface and flashing technique, the EP, as an alternative to the RCP and ZP. Flashing rows and columns of the character matrix of the RCP were replaced by flashing squares located upon the outer edges of the character matrix in the EP. The positions of these squares alternated between lower and upper edges of columns; between left and right edges of rows to denote a target in that row or column when illuminated. The EP can be appropriate for disabled people if they have an ability to slightly control their eye movement. The distance between adjacent flash edge points in the EP is larger relative to the distance between adjacent flash characters in ZP and RCP. The EP has been evaluated and it is significantly improved the online performance accuracy and the user experience relative to the RCP and ZP. This improvement was confirmed in different studies.

3. The design of a portable P300-based Brain-Mobile Interface (BMI) framework that employs the EP on a mobile phone device. The EP is applicable upon

devices with a small screen size because it provides more space between flash edge points and increases the number of flash characters on the interface. Moreover, the EP and RCP have been evaluated on the BMI, and the EP significantly improved the online performance accuracy and the user experience relative to the RCP.

1.4. Organization of the Dissertation

The remainder of this dissertation is organized into seven chapters. Chapter 2 presents a brief background of BCIs, BCI common components, Event-Related Potentials (ERPs), ERP deflections and the components that contribute to those ERP deflections are introduced, including the P300 component, and applications of the P300-based BCI. Chapter 3 introduces the related work in the P300-based BCI area for this research, and this chapter is divided into the work related to the row-column speller paradigm and to the work related to other speller paradigms.

In Chapter 4, the Zigzag Paradigm (ZP) approach is explained. This chapter describes the Emotiv EEG which is used for data acquisition. Also, the ZP visual interface design and visual stimulus design are depicted then the experiment procedure and classification process are described. The last sections of this chapter present the ZP experiment results and discussions. Chapter 5 presents the Edges Paradigm (EP) as a new P300 BCI by presenting the EP visual interface, visual stimulus, experiment procedure, preprocessing and classification, and presents the results of this chapter study.

Chapter 6 presents a comparative study between the row-column paradigm (RCP), ZP, and EP, explains the study procedure, and presents the results with the discussion. Further, this chapter compares ERPs elicited by target, target flanker, and non-target non-flanker flashes in each paradigm. Chapter 7 describes the P300-based Brain-Mobile Interface (BMI), visual interface, stimulus technique, procedure

for the mobility experiment by using a wheelchair, and presents the experiments detail results with the discussion. Chapter 8 provides a general conclusion and some proposed future work which could be conducted in this research area.

CHAPTER 2. BACKGROUND

This chapter presents and introduces an overview for Brain-Computer Interface (BCI), the general functional components of any BCI system, such as data acquisition, preprocessing and classification, and the application program's interface that allow the BCI to interact with the external device or application. Also, this chapter defines the Event-Related Potentials (ERPs) and some ERP types, such as the P300 component, which is used in this research. The last section of this chapter describes the P300-based BCI and some of its applications, where the P300-based BCI speller is the main concern of this research and is used to test and evaluate the new P300 BCI paradigms designed in this research.

2.1. Brain-Computer Interface (BCI)

Communication is very important for people, who can communicate to one another and interact with the environment to accomplish their daily activities and attain their needs. Human-Computer Interaction (HCI) research aims to design and implement efficient interactive interfaces between users and the application's software within computers, mobile phones, or any other devices. The able-bodied can interact with these interfaces by neuromuscular movement, while paralyzed individuals cannot.

A Brain-Computer Interface (BCI) is a non-muscular communication channel between a user's brain and an external machine [96]. In detail, BCI is used to translate the input of Electroencephalography (EEG), digitally recorded via electrodes on the user's scalp, into output commands that control external devices. BCI is a very active and rapidly growing research field, falling within the theme of complex system, drawing together topics from psychology, neuroscience, computer science, and mechanical and electrical engineering [97]. Each field is concerned with specific aspects of the BCI framework, such as signal processing, interface design, machine learning, physical

materials and hardware, or brain neuronal activity. The collaboration between all of these fields is very important to designing and creating efficient BCIs.

BCI design should take into account the needs of the target users, paralyzed, where the brain interface should be simple, easy, clear, intelligent, and comfortable. So, a designer should define the specifications for each object located on the interface, such as the object color, size, font, and style, and place object with respect to the location of other objects.

2.2. Functional Components of BCI

As illustrated in Figure 2, a BCI system includes three stages: signal acquisition, signal processing (signal preprocessing and translation), and device or application interface. To translate the brain signals into commands, these signals should be preprocessed and extracted to the features with suitably formatted structure to identify the pattern of the brain activity via a classification algorithm. This pattern is then converted to commands passed to the device or application interface, where each command corresponds to a specific predefined pattern of brain activity.

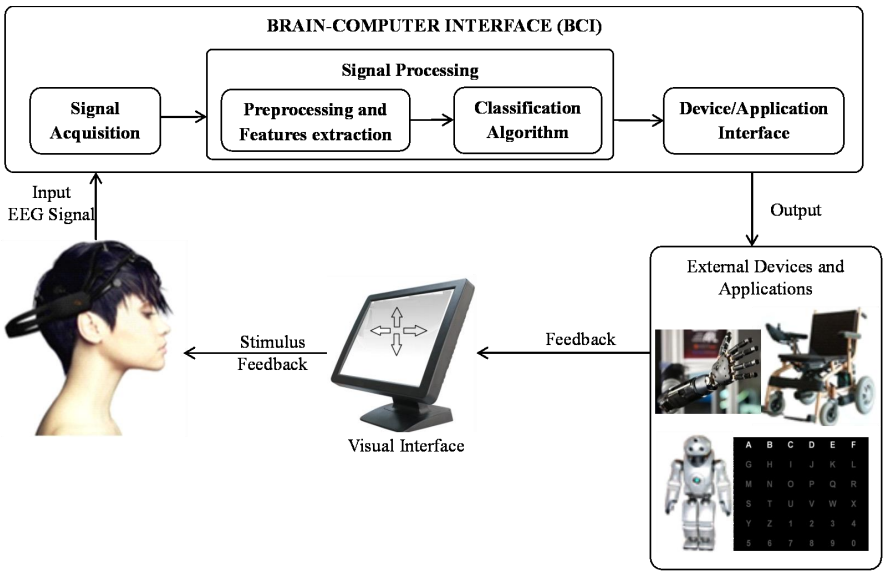

Figure 2. Common functional components of BCI.

2.2.1. Signal Acquisition

Brain signals are one of the most critical things for BCIs, as these signals are used as an essential input to control external devices or any kinds of communication. The brain signals acquisition is the first component in a BCI and can be measured by three techniques:

1. **Invasive BCI:** this technique measures brain electrical activities through brain implanted subdural or depth electrodes, i.e., cerebral cortex. This technique measured the highest quality signals required in advanced BCI applications, such as restoration of vision [21, 55]. There are a set of disadvantages of this technique, being expensive, risky, procedurally complex, difficult to setup, and requiring surgery. Electrocorticography (ECoG) is an example of invasive BCI device.

2. **Partially invasive BCI:** this technique measures brain electrical activities via implanted electrodes upon the surface of the dura, a membrane between the skull and the brain. The signals recorded are a high in quality. Partially invasive BCI requires surgery involving risk and a complex procedure albeit a simpler procedure with less risk than the invasive technique, which introduced above.

3. **Noninvasive BCI:** this technique is the most common brain signal acquisition technique. Electroencephalography (EEG) is one of the most popular real-time inexpensive devices used in noninvasive BCI technique, which was discovered by Hans Berger [8]. The EEG records brain electrical activity via electrodes placed at specific locations upon the scalp often according to the International 10-20 system [85]. Event-Related potentials (ERPs) are derived from EEG. This noninvasive technique is the easiest and safest technique, but recording signals of

a lower quality by comparison with the aforementioned techniques, the bone and tissue between the electrodes and source generators also compromising spatial resolution. This research uses an EEG device, the Emotiv EEG headset.

Most new EEG devices contain an analog-to-digital signal converter to record the signal digitally, EEG data. Also, the EEG device contains an internal digital signal processor that performs oversampling, and digital bandpass and notch filtering to the EEG data in real-time. The EEG signal reflects rhythmic brain activity, often analyzed into five different frequency bands: delta (0.5-3 Hz), theta (3.5-7 Hz), alpha (8-13 Hz), beta (13-30 Hz), and gamma (30-70 Hz) [4].

2.2.2. Preprocessing and Features Extraction

Raw EEG data is typically unsuitable for classification, being contaminated by different artifacts, such as eye movement, muscle and body movement, respiration, cardiac signals, and scalp skin sweating [3, 26, 52]. Preprocessing EEG data and features extraction is very important to convert the EEG data to meaningful features for the classification algorithm.

Many artifacts within the EEG data make the discrimination between the brain evoked potentials based on a target event, e.g., visual flash, and non-target events very difficult. Therefore, common average referencing (CAR) for each EEG data channel (i.e., electrode), further filtering for the EEG data, and winsorizing the EEG data to removing the EEG data outliers are required to remove unwanted noisy sources to improve signal-to-noise ratio (SNR) and enhance the EEG data [46].

Signal processing aims to reduce the raw EEG data dimensions by channel selection with respect to the decimation as necessary, reducing the computational cost and time of classification and enhancing the speed of performance. Subsequently, the preprocessing EEG data is epoched into a meaningful data reduction of time-amplitude features, i.e., segments or epochs, as input to the classification.

2.2.3. Classification Algorithm

The classification algorithm aims to perform a translation of the extracted features into an equivalent feature patterns processed by using pattern recognition to identify the user's commands [59]. In most BCI systems, the classification component is divided into offline and online classification sessions. The offline or training classification session is used to build a classification statistical model (i.e., coefficients) for each individual user depending on certain feature patterns for the calibration dataset gathered during the target and non-target sequence stimulus presented to the user on a visual interface. Thereafter, the online or testing classification session was performed to find the equivalent subject's commands for a set of extracted features in real-time that depend on the classification model. Several classification algorithms are used effectively in BCIs, such as Bayesian Linear Discriminant Analysis (BLDA), Stepwise Linear Discriminant Analysis (SWLDA), Support Vector Machine (SVM), and Fisher's Linear Discriminant Analysis (FLDA).

Concerning classification algorithms, SWLDA, peak picking, area, and covariance, have been shown to operate better under difference circumstances [25]. Hoffmann *et al.* found that the BLDA algorithm is superior to FLDA algorithm in regards to the accuracy and bitrates [46]. Krusienski *et al.* found that SWLDA and FLDA are significantly better than linear support vector machine (LSVM), Pearson's correlation method (PCM) and nonlinear Gaussian kernel support vector machine (GSVM) [56]. Also, the LSVM is significantly better than PCM.

Another study did not find statistically significant differences among SWLDA, FLDA, BLDA, LSVM, and nonlinear GSVM in regards to the accuracy [2]. In contrast, BLDA has demonstrated a smaller divergence in errors as compared with several other classifiers, such as linear discriminant analysis (LDA), SWLDA, support vector machine (SVM), neural network (NN), and feature extraction (FE) [66].

In summary, Fisher's Linear Discriminant Analysis (FLDA) algorithm has been shown to outperform a number of classifiers [56]; an extension of FLDA, the Bayesian Linear Discriminant Analysis (BLDA) algorithm, has been shown to outperform FLDA and other classifiers [46, 66]. BLDA was, therefore, the classification algorithm adopted throughout this dissertation.

2.2.4. Device/Application Interface

A device controller module aims to establish a communication between the classification and external device. Accordingly, this module converts the classification output to the action commands that control external device in the real-time and concurrent sends feedback to the user.

2.3. Event-Related Potentials

Event-Related Potentials (ERPs) are specific waves of brain electrical potentials generated during or after a sequence of external stimuli (sensory stimulation) or internal (motor imagery) thought. The EEG device, via electrodes at different locations on the scalp, is used to derive ERPs. As shown in Figure 3, an ERP waveform consists of a series of positive and negative voltage deflections [63].

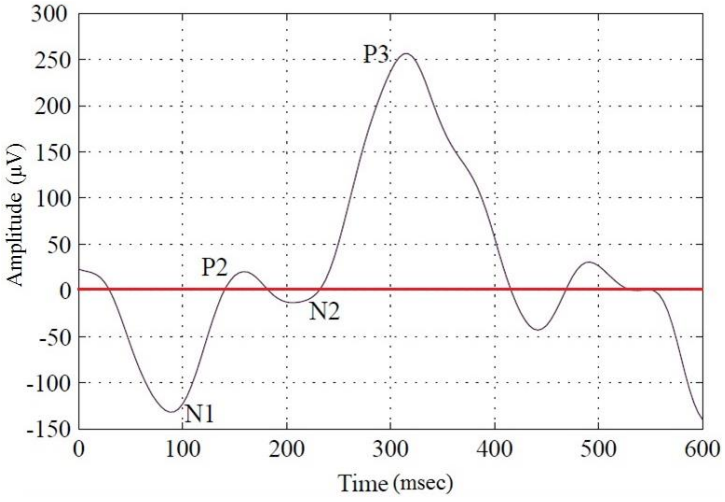

Figure 3. ERP deflections [45].

ERP deflection labels start with a letter P (Positive peak) or N (Negative peak), followed by the time of occurrence in milliseconds in post-stimulus onset, or peak's ordinal position [63]. For example, N100 or N1 are the same ERP deflection, where N1 is a first negative peak that occurs on the ERP. Some ERP deflections are shown in Figure 3, such as P1, N1, P2, N2, and P3.

2.4. BCI Approaches

The noninvasive BCI systems for communication depend on the ERP. This ERP can be generated by the following approaches:

1. **Motor imagery:** this approach does not depend on any external sensory stimulations event, but on the user's mental motor imagery tasks (thinking) to perform a specific and limited muscle movement activity, and detect changes in brain signals from the motor cortex during different imagined movements. For example, the imagination of hand movement to the right or to the left [31].

2. **Steady State Visual Evoked Potentials (SSVEP):** this approach depends on a visual stimulus. The ERP response is recorded through scalp-posterior occipital electrodes, situated over the primary visual cortex. The SSVEP-based BCI presents a set of simultaneous visual stimuli flashing objects – each object flash flashing on and off at a unique frequency – while a user's eyes focus on a target object [57]. The brain generates specific brainwave with a frequency that is the same as the target object frequency.

3. **P300:** this approach depends on the ERPs derived from EEG gathered during the presentation of a sequence of sensory stimuli. For example, P300, a positive peak amplitude component in the ERP that appears with a latency of approximately 300 ms post-stimulus onset of the target object, was discovered by Sutton *et al.* in 1965 [87]. However, P300 is one of the most important

ERP components for BCI research being readily elicited with a short training session. All BCI paradigms developed in this study were based on this P300 component, as is termed here P300-based BCI, which is now introduced.

2.5. P300-based BCI

P300 BCI is defined as a BCI using the EEG input associated with the elicitation of the P300 component in response to stimulation, such as visual flashes, to issue output commands. A P300-based BCI is reliant upon intermittent flashes and uses the principle of an oddball paradigm, where some defined choices display on a screen in front of a user, and the stimuli are presented alternately and randomly. The user focuses gaze on one choice, termed the target, then the P300 potential is elicited as a result of the target properly of the stimulus.

P300-based BCI systems are based upon sensory stimulation, which can be visual, auditory, or tactile [6, 13, 35]. Sensory stimulation evokes electrochemical events within the brain, which in turn cause scalp potentials that are measured with an EEG device via electrodes at different locations on the scalp, as is used to derive P300. Many researchers are interested in working with P300-based BCI systems, because the P300 component amplitude can be reliably measured and easy to elicit from the scalp with an inexpensive EEG device. In addition, P300-based BCI systems do not require a long training session, as mentioned above.

In the last two decades, several P300-based BCI applications have been proposed within different domains of our daily life. The following proposed applications are some examples of P300-based BCI:

1. Brain-Actuated Wheelchair: there are many studies that design a wheelchair that relies on a P300 [48, 58, 78]. For example, the visual wheelchair interface [48] allows disabled people to control a wheelchair movement to specific locations and directions by translating the target selection to the motor commands.

2. Virtual Smart Home: Guger *et al.* proposed a virtual smart home controller based on the P300 ERP component [40]. The different control elements displayed on the interface, such as turning light off/on, opening/closing doors and windows, switching TV channels, etc.

3. NeuroPhone: Campbell *et al.* proposed the first P300 BCI system designed specifically for mobile device [16]. This system allows neural signals to control mobile phone applications, such as call a contact number from the phone address book by selecting one target flash contact image.

4. P300-based BCI Speller: P300-based BCI speller (or BCI speller) is one of the most successful applications based on the P300 ERP component, and this application has shown a high accuracy performance in several studies. A BCI speller aims to help disabled people to type text on a computer by selecting one alphanumeric character at a time. The pioneering work of Farwell and Donchin [25] displayed 36 characters into a 6-by-6 matrix in a row-column paradigm (RCP). The rows and columns are flashed alternately and randomly on the screen. The user focuses on the target character and counts the number of times the target flashes. The character located at the intersection of the row and column, which elicited the largest P300 amplitude, is the character identified and should be the target.

CHAPTER 3. RELATED WORK

Having already defined the adjacent, crowding, and fatigue problems of the Row-Column Paradigm speller (RCP) and the objectives of this study (Chapter 1), as well as having introduced the general background of the BCI and some of the BCI applications (Chapter 2), this chapter now turns to the RCP and its related studies in more detail.

A brain-computer interface (BCI) is not only used by disabled users, but also it may be used by healthy users to improve their interaction with the external world in specific situations and applications [31]. Since the BCI research field evolution within the last two decades, it is still poorly explored by researchers, probably due to the essential complexity of this multidisciplinary research topic [31, 71, 95]. Several studies proposed some improvements to the RCP presented in the first part of this chapter, such as the RCP visual interface and stimulus improvements. The last part presents other that studies proposed new P300-based BCI speller paradigms rather than the RCP.

3.1. Row-Column Paradigm (RCP)

This research intends to build upon prior developments of the P300 speller, particularly the aforementioned RCP, which is introduced in more detail in what ensures. With the RCP [25], oddball sequences of visual letter stimuli are employed that contain rare unpredictable target stimuli interspersed amongst a series of non-target stimuli. The RCP is designed as a 6-by-6 matrix of 36 characters. Six rows followed by six columns are briefly flashed in a random order. The user is instructed to focus on the target character and to count the number of times that the target character flashes. There are 12 possible events (six row and six column flashes) and only 2 events are relevant to the target character (i.e., the possibility of flashing the target character is 2/12). The P300 amplitude is measured after each flash. After a

number of flashes, a classification algorithm identifies the row that elicited the largest P300, the column that elicited the largest P300, and, in turn, the target character at the row-column intersection. The general approach of this widely-used successful RCP is adopted here.

P300 is an endogenous component not significantly affected by the stimulus attributes [82], but the exogenous stimulus attributes, such as characters' color, size, distribution, duration time, etc., can affect the perceptual response [74, 89]. Several modifications were intended to improve RCP online classification performance and user experience by reducing the effects of the aforementioned RCP problems, such as adjacent, crowding, and fatigue problems. Some BCI researchers replaced the RCP by new BCI speller paradigms, and some other researchers improved the RCP performance and keep the RCP matrix.

3.1.1. RCP Visual Interface

In Salvaris and Sepulveda [81], various changes to the RCP visual interface are explored as well as their effects on classification accuracy. Changes to the characters' size, the distance between the characters were evaluated. A systematic evaluation of RCP has revealed that increasing matrix characters' size or distances between matrix characters yielded better classification performance. Such an approach was thought to alleviate the crowding problem, in accordance with Bouma's law [12] that identification of a stimulus improves as a function of the eccentricity between the target stimuli and flanking stimuli; a law that accordingly generalizes from cognitive performance to classification by BCI. However, reducing the size of characters, or the distance between matrix characters, conversely reduced classification performance, so this approach was arguably confounded by factors other than distance, thus rendering the reduction in character size ineffective in alleviating crowding (i.e., number of characters surrounding a character) and adjacency (i.e., distance between neighbor

characters) problems. Further, the previous results agree with Fazel-Rezai results [27], which shown that 60% of errors in detecting target character occurs in adjacent rows and columns to the target ones.

Further corroboration of Bouma's law, in a BCI context, was thus sought by using shifting to increase the distance between target and flanking matrix characters in the Zigzag Paradigm (ZP) relative to RCP. This shifting also addressed the crowding problem, for most characters, by reducing the number of other characters surrounding a character; critically the target character. Also, adding an edge point as a stimulus beside each row and column in the RCP matrix doubles the distance between target and flanking edge points in the Edges Paradigm (EP) relative to RCP. Furthermore, adding these edge points reduced the number of flash objects surrounding any object.

The size of RCP matrix has not been shown to significantly influence accuracy [1, 83], so the traditional size of character matrix (6-by-6) is used in this work for both proposed speller paradigms, ZP and EP.

3.1.2. RCP Visual Stimulus

Variants of the traditional visual stimulus, a flash, used in the RCP, have been investigated and tested in several studies. Any flash design should follow existing findings from the psychology and neuroscience to make this flash design more effective on the ERP components. Each flashing technique has been shown to produce different levels of classification accuracy. An approach to the crowding and adjacency problems has been the Single Character Paradigm (SCP), which only flashes one single character at a time [39], as shown in Figure 4. The SCP was intended to increase the P300 amplitude thus attaining a higher overall accuracy than the RCP. Compared with the RCP, the SCP increased the P300 amplitude. However, such improvements in accuracy were not obtained and, of more concern, the communication rate (i.e., number of selection characters per minute) was reduced.

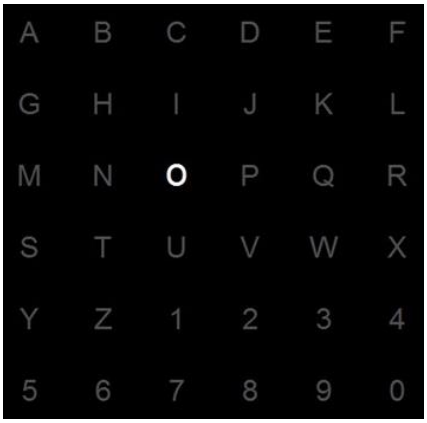

Figure 4. The Single Character Paradigm (SCP).

Townsend *et al.* introduced the Checkerboard Paradigm (CBP) [90], depicted in Figure 5, adopted a different technique for addressing the adjacency problem by flashing 6 non-adjacent characters simultaneously. Also, the CBP increases the matrix dimension to a 9-by-8 matrix of 72 characters. While the CBP showed improvements in classification accuracy over RCP, neither the SCP nor CBP improved upon the communication rate and accuracy of the RCP, or reduce the crowding problem. Other extended approaches were intended to enhance the CBP, such as suppressing characters surrounding targets from ashing during the offline session [34], reducing the total number of flashes [91], or even using a hybrid spelling approach that combined electrooculogram (EOG) with EEG [77]. While these extensions improved the communication rate and the bit rate, online classification accuracy went unimproved over the performance demonstrated with the CBP.

In a variant of RCP, an approach to the crowding problem was to replace characters with familiar faces (FF) [53], as augmented P300 amplitude, and significantly improved classification performance. This promising finding suggested that the crowding problem could be alleviated by reducing the physical similarity between characters in the matrix. The FF used the same face to flash all row and column

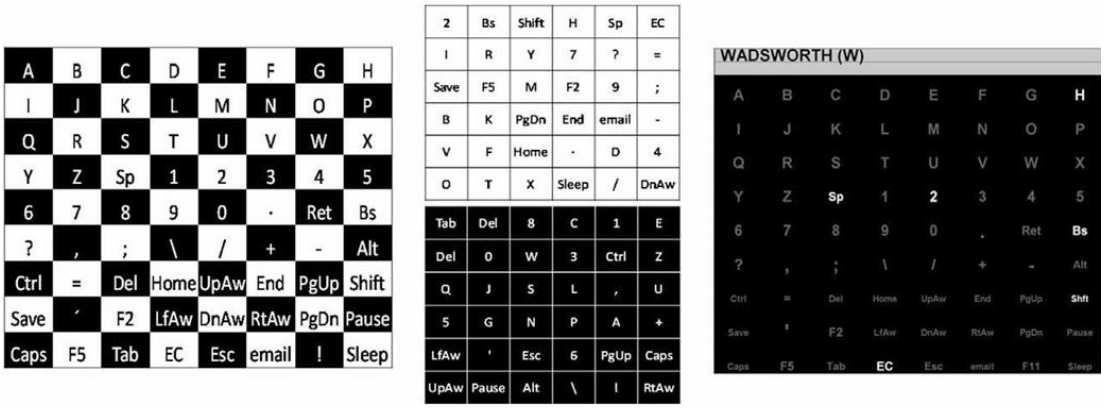

Figure 5. The Checkerboard Paradigm (CBP) [90].

characters as illustrated in Figure 6, which makes a difficult to distinguish between a target and flankers characters flashes. Other approaches were changed the standard flash colors, gray and white, to another one [47, 88] to reduce the crowding effect. These approaches, the FF and changing the flash colors, did not increased the distance between adjacent characters and reduced the number of characters in a visual spatial crowding as well.

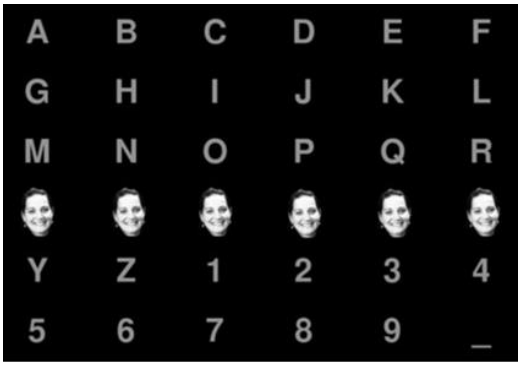

Figure 6. The characters with flashing familiar faces (FF) [53].

Instead of flashing characters into rows and columns, some studies designed alternate flash pattern approaches to decrease the number of flashes needed to identify a target character and speed-up the communication rate as well. Jin *et al.* designed

four flashing techniques using 9-, 12-, 14-, and 16-flashes to identify a target character for a P300 BCI speller based on a 7-by-12 matrix [49, 50], while this matrix requires 19 flashes (7 rows and 12 columns) in the RCP. However, the results revealed that the online classification performances of the 16-flashes and 19-flashes patterns are equal to each other and better than remaining patterns. According to these results, using the same number of flashes as original flashing technique (rows and columns) is adopted in this work. More specifically, the number of flashes in the RCP as well as the new speller paradigms, the ZP and EP, is the number of rows multiplied by number of columns.

The effect of a different stimulus-onset asynchrony (i.e., SOA; the time between the onsets of the two successive flashes) was also investigated for the RCP and conflicting results were reached. A short SOA of less than 200 ms commonly used in different spellers [84, 90, 77, 98, 72] has engendered a higher data transfer rate. Turning to the influence of SOA on accuracy, a shorter SOA has also been shown to produce a higher online accuracy [68, 83]. In contrast, Farwell and Donchin found a longer SOA increases the online classification accuracies [25, 61], so there is a discrepancy between the results of the previous studies. To increase the communication rate, a short SOA (120 ms) is used in this research for the RCP, ZP, and EP. The SOA duration is divided into a short inter-stimulus interval (i.e., ISI; the time between the flash termination and the onset of the next flash) (50 ms) and a short yet supraliminal flash duration (70 ms).

For any P300 speller paradigm, the double-flash problem may happen when the target character flashes twice consecutively, which can reduce the P300 amplitude for the second flash of the target character which reduce the overall performance accuracy for a speller [90]. Serby *et al.* flashing technique [84] is used in this work to address the double-flash problem and prohibited that the target flashed twice in succession.

3.2. New P300 BCI

Several promising new BCI speller paradigms have been developed, and some of these paradigms do not require eye movement to the target character (covert attention) [10, 73, 92, 93], where other paradigms are required to focus on a target character to select it (overt attention) [28, 74, 92, 98]. In several new paradigms, [10, 28, 73, 92, 93], the target character is selected in two stages. In the first stage a region containing multiple characters is selected, and then, in a second stage, each character in that region is distributed in a new window, from which the target character is then selected.

The RCP provides a higher accuracy in overt attention mode relative to the covert attention mode [14, 33, 92]. Treder *et al.* developed and evaluated three of two-stage BCI speller approaches based on covert attention mode [93], where the user only needs to fixate the center of a visual speller and covertly select the target character. Of these two-stage approaches, the Center Speller was established as the most accurate performance relative to the Hex-o-Spell and the Cake Speller.

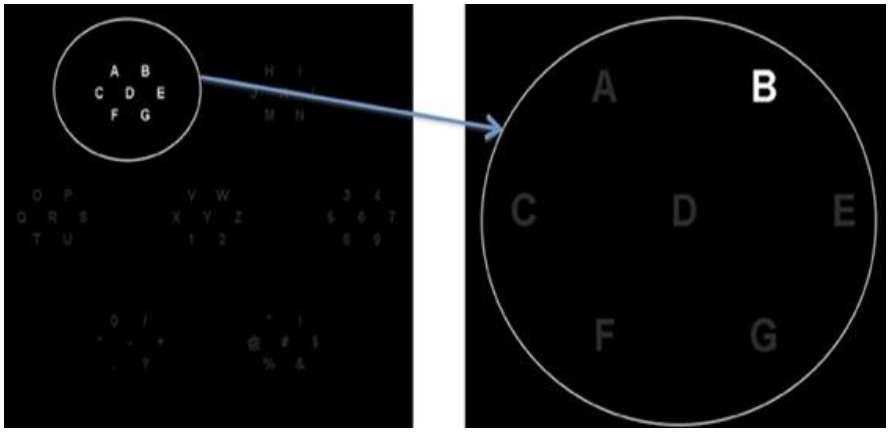

Figure 7. A region-based BCI speller paradigm (RBP) [28].

A region-based paradigm (RBP) is another type of a two-stage P300 spellers introduced by Fazel-Rezai [28], as shown in Figure 7, and it is in the same line of an

overt Hex-o-Spell discussed in [92] and introduced in [10] with some changes. The RBP and the most two-stage speller paradigms increased the number of characters relative to the RCP, and increased distance between those characters (or regions) as improved accuracy by alleviating the crowding and adjacency problems respectively. These paradigms thus demonstrated improvements in accuracy over RCP, yet communication rate was slowed by the two-stage nature of the process. The objective of this work was thus to improve accuracy without slowing communication rate in a single-stage interface: the ZP. Though the EP works as a two-stage speller paradigm, but this speller use one window only without changing the characters and edge points locations on the EP interface to reduce the memory load in comparison with other two-stage speller paradigms.

An investigation is thus conducted – with different P300 speller's – which assessed BLDA classification performance and user experience in the comparison of a single-stage ZP, a two-stage EP, and a single-stage RCP. Short flash durations and ISIs are used. This research was intended to assess how well ZP's shifting and EP addressed the crowding, adjacency, and fatigue problems that affect RCP.

CHAPTER 4. THE ZIGZAG PARADIGM (ZP)

This chapter describes a new P300-based BCI speller paradigm, called the Zigzag Paradigm (ZP), and presents the ZP experiment results. The ZP is designed to address the RCP problems mentioned in the previous chapters. The sufficiency of ZP's solution to adjacency and crowding problems can be evaluated by speller performance, while whether the improvement of the interface reduces the fatigue problem can be assessed by subjective ratings. Accordingly, an empirical investigation was conducted to evaluate the predicted improvements in performance and user experience with ZP.

4.1. Methods and Materials

4.1.1. Participants

14 university students participated, of which 5 were excluded from data collection due to frequent disconnection from the Emotiv EEG apparatus, as occurred only with individuals who had long, coarse, or dense hair; a known problem for such individuals particularly when using the saline electrodes employed in the current investigation [20, 24]. The remaining 9 volunteers were aged 22 to 34 years (mean: 28 years; all male). All reported intact vision, no neurological conditions, and English as their first language. The study received ethical approval from the North Dakota State University Institutional Review Board and each participant gave informed written consent in accordance with the Declaration of Helsinki.

4.1.2. Hardware and Data Acquisition

Data were recorded via the "Research Edition" of the Emotiv EEG wireless headset, [20, 24] at 128 Hz in a 0.16-45 Hz bandpass from saline scalp electrodes positioned at the selected scalp sites approximating the International 10-20 system of electrode locations [85] depicted in Figure 8.

EEG data were acquired using the EmotivEEG Headset Toolbox written in MATLAB [36]. The interface design, preprocessing, feature extraction, and classifi-

cation algorithm were custom routines written in MATLAB.

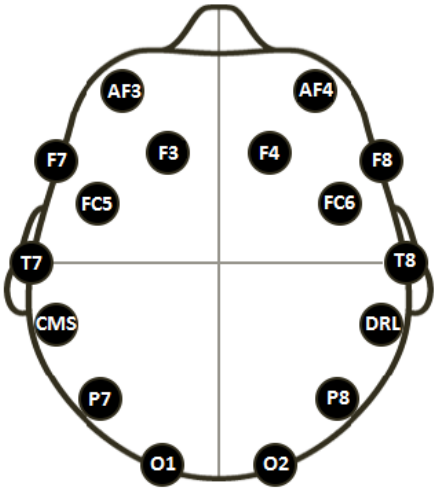

Figure 8. Emotiv EEG electrode locations [24].

4.1.3. Visual Interfaces Design

Both the RCP and the ZP interfaces were divided into a small upper part and a larger lower part (See Figure 9). Specifically, the small top part was identical in both interfaces, and consisted of two text boxes - one for input, the other for output - and a start button that is pressed to run the speller. Contrastingly, the large lower part was different for the two interfaces. In the RCP, the large lower part included a 6-by-6 matrix with 36 alphanumeric characters evenly distributed within an area of $h \times w$ centimeters (cm) (our design is 12.7×12.7 cm). The distance between two adjacent characters located on the same row or column was d cm (See Figure 9(a)), and $\sqrt{d^2 + d^2}$ cm was the distance between the two adjacent characters located on a different row and column (See Figure 9(a)). In the RCP, each character is surrounded by 3, 5, or 8 characters, as shown in Figure 9(a). In the ZP, after shifting the even number of rows to the right by $d/2$ cm, the width is increased to $w + d/2$ cm (Figure 9(b)). In the ZP, the distance between two adjacent characters in the same row was still d cm, with $\sqrt{d^2 + (d/2)^2}$ cm between two adjacent characters located on different rows. This shifting reduced the number of characters surrounding any

character, which then ranged from 2 to 6 (Figure 9(b)).

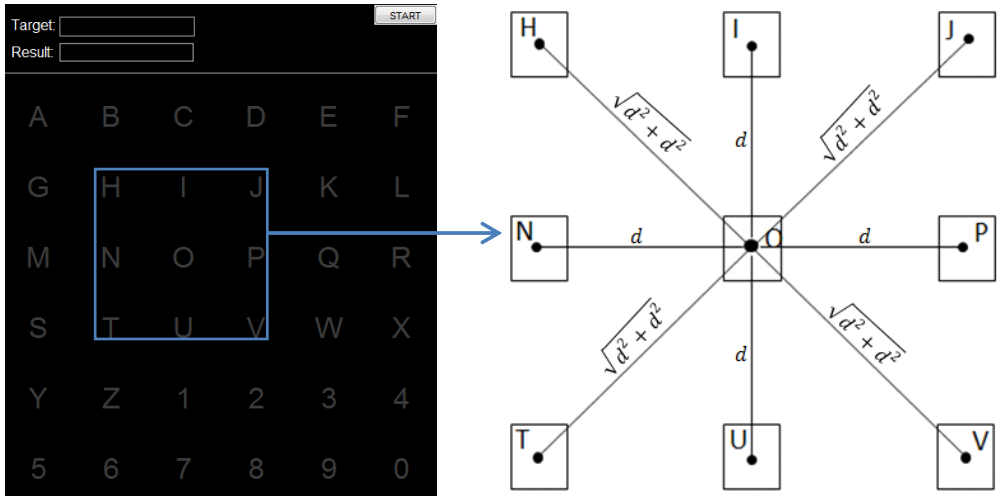

(a)

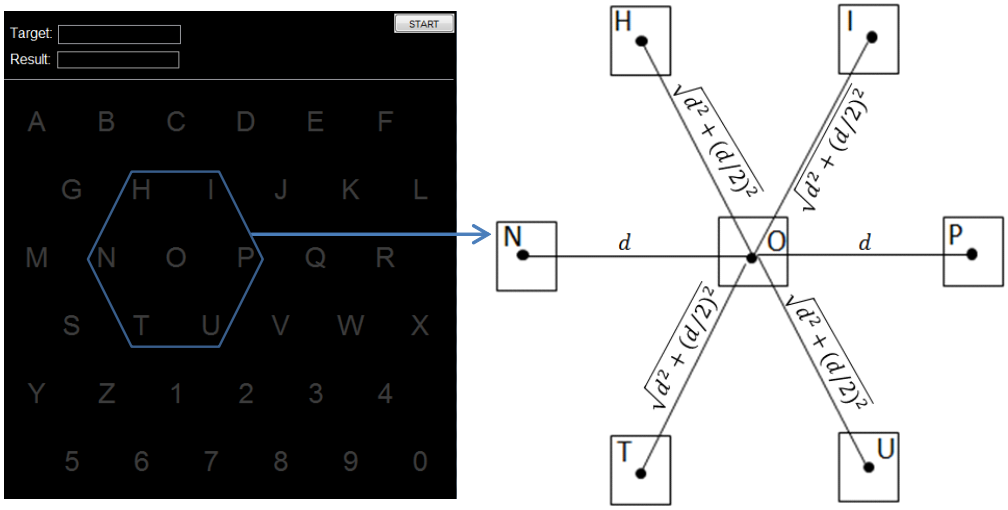

(b)

Figure 9. (a) The RCP visual interface, (b) The ZP visual interface.

The characters located on the zigzag column were the same as characters located on the straight column in RCP. Both paradigms used the same flashing technique and classification algorithm.

4.1.4. Visual Stimulus Design

The visual stimulus used in the study was a flash, as shown in Figure 10. To resolve the double flash problem mentioned in the Introduction, for both spellers (RCP and ZP), each block consisted of 6 row or 6 column trials (flashes), and it was prohibited that the same row or column flashed twice in succession [84].

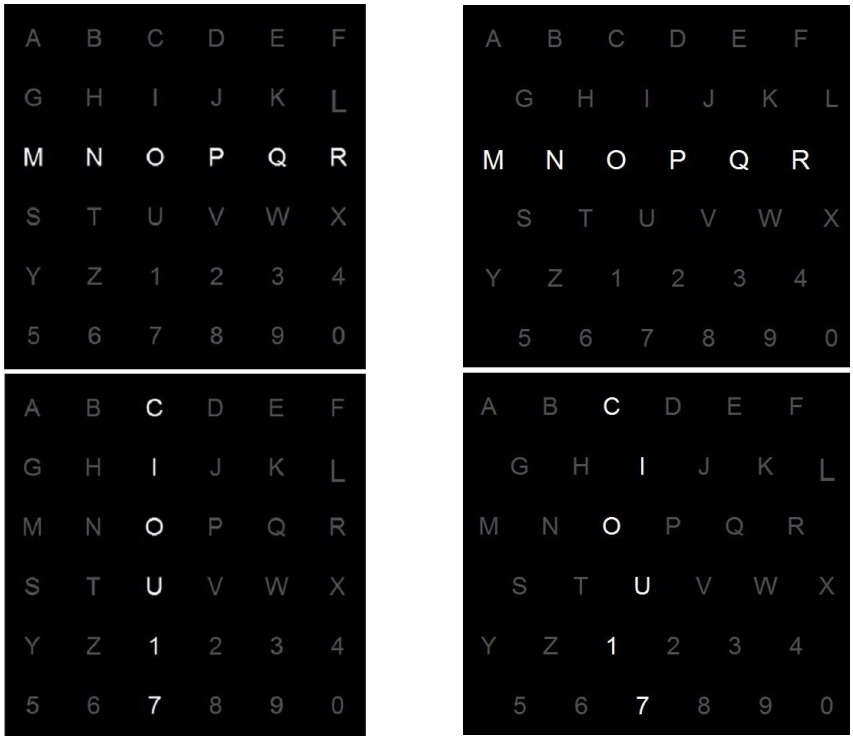

(a) (b)

Figure 10. The row and column visual flashes for the RCP (a) and ZP (b)

The order in which each of the rows or columns were flashed within a block was otherwise randomly permuted, as illustrated in Figure 11. There were 24 blocks per target (12 row blocks, followed by 12 column blocks). For each target, each row was thus flashed a total of 12 times and each column was flashed a total of 12 times, i.e., (12 row blocks * 6 flashes) + (12 column blocks * 6 flashes) = 144 flashes per character, with the target flashing one time on each block, such that the target flashed 12 + 12 = 24 times on all blocks, and non-targets flashed 144 - 24 = 120 times. As

depicted in Figure 11, the inter-stimulus interval (ISI) was 50 ms, and the stimulus-onset asynchrony (SOA) was 120 ms. Each block thus lasted 120 * 6 = 720 ms. 24 blocks, containing in total 144 trials, were needed to select one target character, such that a net time of 120 * 144 = 17280 ms was needed to select each target.

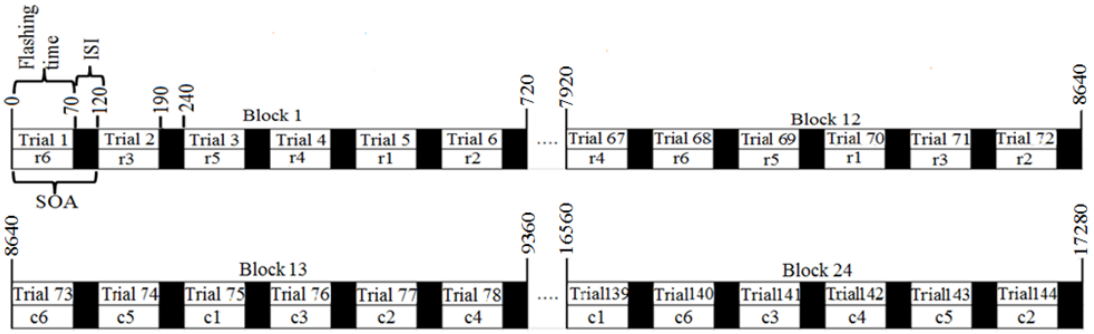

Figure 11. Flashing sequence design for one target character selection (r: row, c: column).

4.1.5. Procedure

Each participant completed a measurement with ZP and a separate measurement with RCP upon a separate day. Each measurement lasted approximately an hour and was divided into two sessions; 40 minutes for the offline session (i.e., collection of calibration data), and 20 minutes for the online session. Whether the RCP measurement or the ZP measurement was conducted on the first day, was alternated between successive participants. Before each measurement, the participant was asked to rate his current level of fatigue on a scale of 1 to 10 (1: no fatigue, 10: severe fatigue). After each measurement, the volunteer completed a post-study questionnaire in which he again rated his level of fatigue, together with the level of comfort (1: uncomfortable, 10: comfortable) and alertness (1: drowsy, 10: alert) that he had experienced during the experiment.

The volunteer sat on a chair in front of the speller displayed on screen of the computer monitor at a viewing distance of 90 cm. Participants were instructed

to focus visual attention on a target symbol, while silently counting the number of times the target character flashed, keeping blinking and muscle movements to a minimum. Volunteers were observed by the experimenter to ensure that they followed the user study instructions and that head, leg, and eye movements were kept to a minimum. All participants were complaint with the instructions throughout. In the offline session, 6 words and a number (LAP, ROD, BAND, FLAG, DRINK, MINUTE, and 9253), as comprised 29 alphanumeric characters, were tested by each participant. The purpose of the offline session was to train the classifier algorithm to build a classification model for each individual participant (i.e., classification coefficient). The online session then used 3 words and a number (SUM, LAMP, BUNCH, and 7492), as consisted of 16 alphanumeric characters, which were used to test the accuracy of the classifier for that participant according to the classification model. Words were drawn from the MRC psycholinguistic database [19] on the basis of having similar, relatively early, Gilhooly and Logie (1980) Age-Of-Acquisition norms [37].

In offline and online sessions, the target word was presented in the target text box for each run, and, one-at-a-time, the current target character was displayed in the 6-by-6 matrix in red for 1.5 sec before the row and column trial flashes ensued. This period prior to the presentation of blocks of trials was intended to permit the participant to shift their visual focus and fixate the target character so they could then count the number of times the target flashes. The Emotiv EEG signals for each single target character were acquired in parallel with the row and column flashes, and both of the EEG raw data and flashes data (row/column flashes sequence, event, target character ...) were stored in two different files, which were then merged into one complete MATLAB file (.mat). Then, the EEG data was converted to a form suitable for the classification algorithm. Figure 12 shows the overall software architecture.

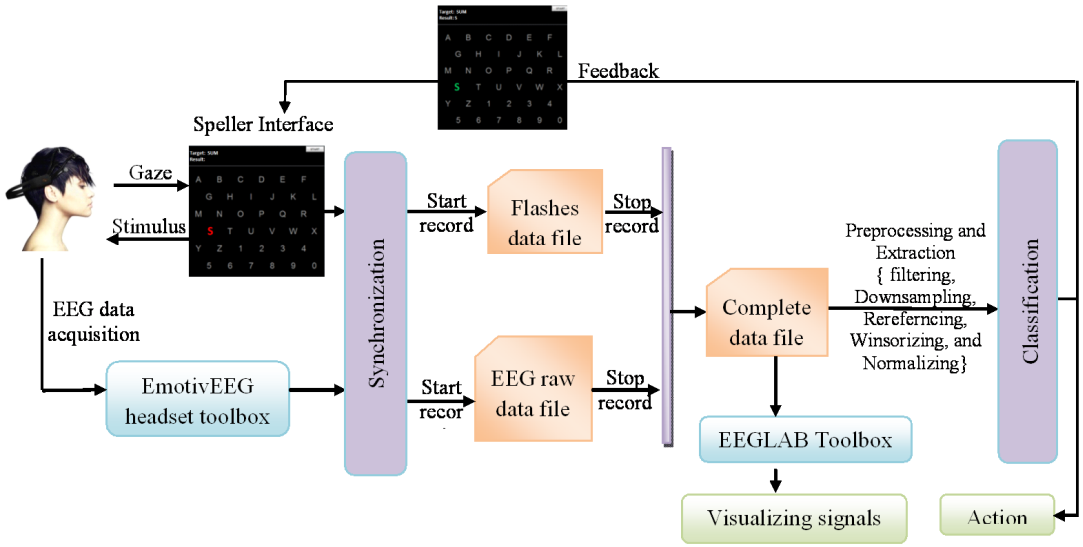

Figure 12. Overall P300-based BCI Architecture.

4.1.6. Preprocessing, Feature Extraction, and Classification

In general, the raw EEG data collected for each single target character was unsuitable for classification, being contaminated by different artifacts (eye movement, muscle and body movement, respiration, cardiac signals, and scalp skin sweating) [3, 26, 52]. Therefore, preprocessing took place for artifact reduction prior to feature extraction.

The Emotiv device digitally-filtered the raw EEG signals in a bandpass of 0.16 to 45 Hz. For common average referencing, the average potential at all 14 electrodes was calculated for each time point, and then the average was subtracted from all data at that time point. Continuous EEG data recorded for each single target character was epoched 0 to 600 ms post-stimulus onset (See Figure 13). There were 144 epochs (i.e., segments) per target character. In other words, a 600 ms time frame of data was extracted following each flash to identify if that flash evoked the P300 component. From the data structure perspective, a segment is a two-dimension matrix with the size of 14 electrodes by 77 time points per segment, where number of time points = (ceil(0.6 * 128)) as each 0.6 sec epoch was recorded at 128 Hz. 5% of the highest

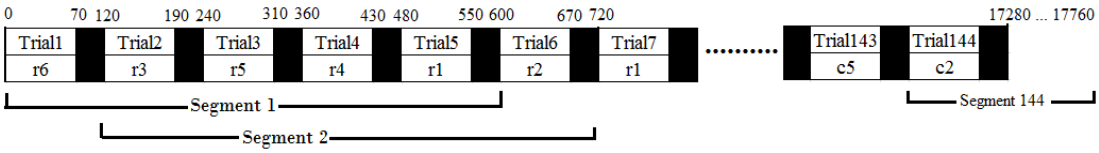

Figure 13. EEG data extraction (segments) for one target character selection.

sample amplitudes (artifacts) for each electrode were reduced to the 95$^{\text{th}}$ percentile amplitude value. Also 5% of the lowest sample amplitudes for each electrode were increased to the 5$^{\text{th}}$ percentile value. This process is termed Winsorizing [46].

Bayesian Linear Discriminant Analysis (BLDA) was employed to identify the target character. For each participant, the classifier was trained on the calibration data collected from the offline experiment. The calibration data contained 144 * 29 = 4176 flashes (24 * 29 = 696 target flashes and 120 * 29 = 3480 non-target flashes). Thereafter, online classification was performed after the EEG data for the 144 row and column flashes were recorded. In general, the classifier ran twice to infer the target character. First, each single row segment from the 72 row segments was classified separately, and the summation of the classification results determined for each row segment over the 12 row blocks was calculated. The row with the highest summation was considered as the target row, as is shown in Equations 4.1 and 4.3. Second, the same process was applied to column segments to identify the target column, as is shown in Equation 4.2 and 4.4. Finally, the character located at the intersection of the target row and the target column was selected as the target character.

$$Total\_BLDA(r_i) = \sum_{n=1}^{12} BLDA(r_i, n) \tag{4.1}$$

$$Total\_BLDA(c_i) = \sum_{n=13}^{24} BLDA(c_i, n) \tag{4.2}$$

$$Target\_Row = max(Total\_BLDA(r_i)) \tag{4.3}$$

$$Target\_Column = max(Total\_BLDA(c_i)) \tag{4.4}$$

Where, r is row segment and c is column segment; i is the row or column number (1, 2, 3, 4, 5, 6); n is the row block number (1, 2, ..., 12) or the column block number (13, 14, ..., 24); $BLDA(r_i, n)$ and $BLDA(c_i, n)$ is the BLDA classification results of row i segment and column i segment respectively for block n.

4.2. Results

4.2.1. Online Classification Performance

As depicted in Figure 14, the pattern of mean percentage classification accuracy suggested that performance was improved with the ZP relative to RCP.

These findings were corroborated by inferential statistical analysis: A paired t-test revealed that the performance improvement produced with the ZP relative to the RCP interface was significant, $t(8) = 4.08$, $p = 0.004$, $\eta^2 = 0.676$ (7/9 showed the effect).

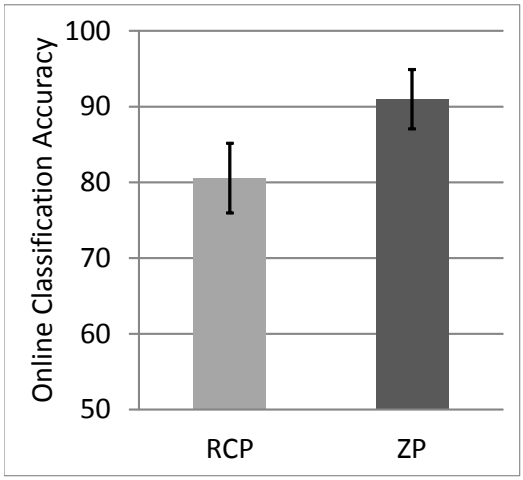

Figure 14. Mean percentage classification accuracy as a function of interface (error bars denote standard error); N=9.

For each paradigm, error distribution matrices were calculated for the 144 selected characters for all volunteers (16 characters * 9 participants = 144 selected characters), as shown in Figure 15. Target characters were denoted by the center cell, showing the number of correctly-selected characters. Other cells contained the number

of erroneously-selected characters. The difference in rows and columns between the erroneously-selected character and the target character is denoted by the cell position. For example, if a participant erroneously-selected a character with the speller, then the error value of the cell position (selected row-target row, selected column-target column) within the error distribution matrix is incremented by one.

The frequencies in these error matrices showed that the adjacency problem was ameliorated with the ZP: As shown separately for each interface in Figure 15, RCP-detected errors totaled 19.4% (28 out of 144), ZP-detected errors 9% (13 out of 144). Whereas 43% (12 out of 28) of these RCP-detected errors were adjacent errors, 30% (4 out of 13) of these ZP-detected errors were adjacent errors. With 75% (21 out of 28) of the RCP-detected errors, and 92.3% (12 out of 13) of the ZP-detected errors, either the row or the column was correctly classified.

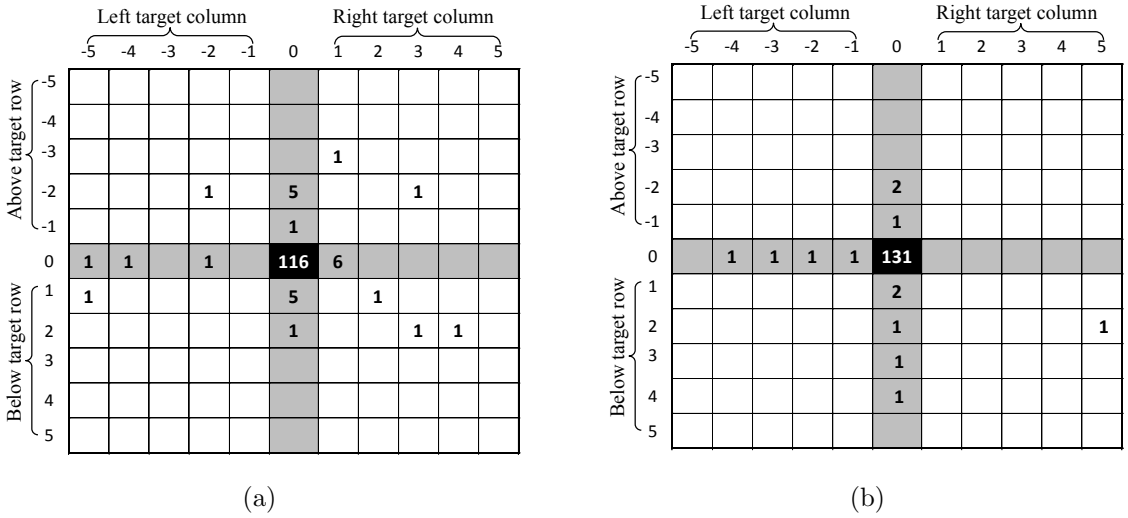

Figure 15. The error distributions matrix of all subjects for 16 selected characters in the online session for the RCP (a) and ZP (b). The center cell indicates the number of correct selections for all target characters.

4.2.2. User Experience

Here the data were questionnaire-assessed subjective ratings of fatigue, comfort, and alertness. The pattern of means illustrated in Figure 16(a) suggested that the ZP

caused relatively less fatigue than the RCP, and that volunteers reported, as depicted in Figure 16(b) that ZP was more comfortable after the experimental session, as well as being more alert with ZP. The subjective rating range is 1 to 10, where 1 indicates the lowest level of fatigue (the best case), while 1 indicates the worst case in comfort and alertness.

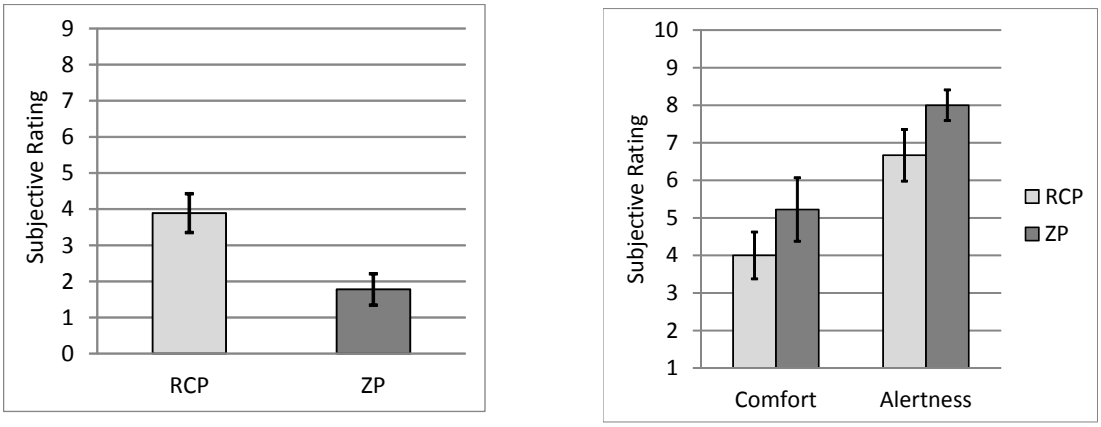

(a) (b)

Figure 16. Subjective rating for all participants (N=9). (a) Mean of the fatigue rating difference before and after the experiment (0:9). (0: lowest level of fatigue, 9: highest level of fatigue). (b) Mean of the comfort, and alertness rating (1:10). (1: lowest level of comfort and alertness, 10: highest level of comfort and alertness).

These tendencies were broadly supported by inferential statistics: Paired t-tests comparing ZP and RCP revealed a significant effect of interface upon fatigue, $t(8) = -3.59$, $p = 0.007$, $\eta^2 = 0.676$ (9/9 showed the effect), and upon comfort, $t(8) = 2.82$, $p = 0.023$, $\eta^2 = 0.498$ (7/9 showed the effect). The effect of interface upon alertness was, however, marginal, $t(8) = 2.31$, $p = 0.050$, $\eta^2 = 0.246$ (6/9 showed the effect).

4.3. Discussion

The results showed that increasing the distance between most characters, reducing the visual spatial crowding through the shifting process (i.e., ZP), decreased the number of adjacent errors. The ZP significantly improved accuracy relative to

the RCP. Also, most participants, overall, found the ZP to be more comfortable and to cause less fatigue.

These findings supported Bouma's law [12] that identification of a stimulus improves as a function of the eccentricity between the target stimulus and flanking stimuli, such that there was a reduction in visual crowding and the effects of the adjacency problem [27] using the new ZP. Which brain processes support the multiple levels upon which visual crowding can occur remain to be identified [94], as does how these processes causally influence the generation of P300 shown here during ZP and RCP. Dissociations have been drawn between the visual system, implicated in perceptual identification, and the visualmotor system, implicated in actions such as grasping a target object amongst multiple objects [15]. P300 generation is assumed to reflect a decision process [75], which could be engaged by processes in the visual system, or in the visualmotor system, or, even, within both systems. In healthy individuals, this visualmotor system is arguably less susceptible to crowding [15] than the visual system, such that vision can guide action effectively in crowded visual environments, e.g., pressing keys upon a small mobile device.

It therefore remains an intriguing empirical question of theoretical and practical value as to whether patients with motor problems, associated with neuromuscular diseases such as ALS, would particularly benefit from the improvements in performance and user experience shown with ZP here. Concerning possible improvements to the ZP indicated by classification performance of the current investigation, for almost all ZP classification errors in the current investigation, either the row or the column was correctly classified (Figure 15(b)). The results of the present investigation have thus given rise to a question that concerns whether the nonadjacent flashes employed in the Checkerboard paradigm [90] might be more effective in the ZP, rather than the flashing rows or columns with the ZP used here. It is to be determined if such

nonadjacent flashing might further minimize the classification errors that confuse the target character with another character in the same row or column.

CHAPTER 5. THE EDGES PARADIGM (EP)

The Zigzag Paradigm (ZP) improved the online classification performance and user experience of the Row Column Paradigm (RCP) by reducing the weakness of the RCP through a shifting process, as explained in Chapter 3. Unfortunately, the ZP increases the interface size relative to the RCP interface. Consequently, the ZP is not suitable for mobile P300 speller (i.e., small screen size). This chapter discusses a novel P300 speller interface developed and evaluated, called the Edges Paradigm (EP). The EP is intended to address the adjacency, crowding, and fatigue issues of the RCP by replacing the traditional row/column flashing with the square flashing in the boundary of a character matrix. This chapter shows the speller interface and stimulus design of the RCP and EP, explains the experiment procedure, lists the preprocessing and classification steps, presents the results of the online classification performance and user experience for the RCP and EP, and discusses it.

5.1. Methods and Materials

5.1.1. Participants

17 neurologically normal university students and employees, who did not suffer from paralysis, voluntarily gave their informed written consent to participate in this investigation, which was approved by the Institutional Review Board of North Dakota State University, in accordance with the Declaration of Helsinki. 3 participants were excluded from the investigation because the Emotiv EEG device became disconnected frequently. These excluded participants had long, coarse, or dense hair insulating the connection between the scalp and the saline electrodes employed in the current investigation [20, 24, 72]. The remaining 14 participants (aged 20-35 years; mean: 27 years; 2 females) all reported English as their first language and all of them corrected-to-normal vision or normal vision.

5.1.2. Hardware and Data Acquisition

EEG was recorded using 14 saline electrodes positioned on the scalp according to the International 10-20 system of electrode locations [85]: (AF3, F7, F3, FC5, T7, P7, O1, O2, P8, T8, FC6, F4, F8, and AF4); these electrodes were embedded within the Emotiv EEG wireless headset. The Emotiv EEG with the "Research Edition" was used for digitized signals at 128 Hz, and then the EEG data were filtered using a 0.16-43 Hz bandpass [24]. The P300 speller systems, EP and RCP, were implemented on a PC using custom routines and EEG data simultaneously acquired onto the same computer via the EmotivEEG Headset Toolbox [36]. All presentation and acquisition software was written in MATLAB 7.14.0.739.

5.1.3. Visual Interfaces Design

The RCP and EP visual interfaces are shown in Figure 17. This figure is annotated with abbreviations for the objects' dimensions and the distances between objects, as elaborated in Table 1, alongside the actual values of these dimensions and distances used in the two interfaces. Both interfaces were divided into a small upper panel and a large lower panel. The upper panel in both interfaces consisted of input and output text boxes and a start button to run the speller. The lower panel of the RCP, depicted in Figure 17(a), included a 6-by-6 matrix of 36 gray alphanumeric characters. The lower part of the EP, illustrated in Figure 17(b), was identical to the lower part of the RCP, except that the alphanumeric characters had a white color and that a gray edge point was added to the left side of row 1, 3, and 5, the right side of row 2, 4, and 6, below column 1, 3, and 5, and above column 2, 4, and 6.

In the RCP and EP interfaces, each character was surrounded by 3, 5, or 8 characters, whereas each edge point in the EP was surrounded by 1 or 2 edge points. The EP implemented a different flashing technique from RCP. More specifically, EP only flashed the edge point rather than the entire row or column, so the distance

between adjacent flash objects was doubled. Although the RCP and EP interfaces and flashing techniques were different, the same BLDA classification algorithm [46, 51, 60, 66, 72] was used.

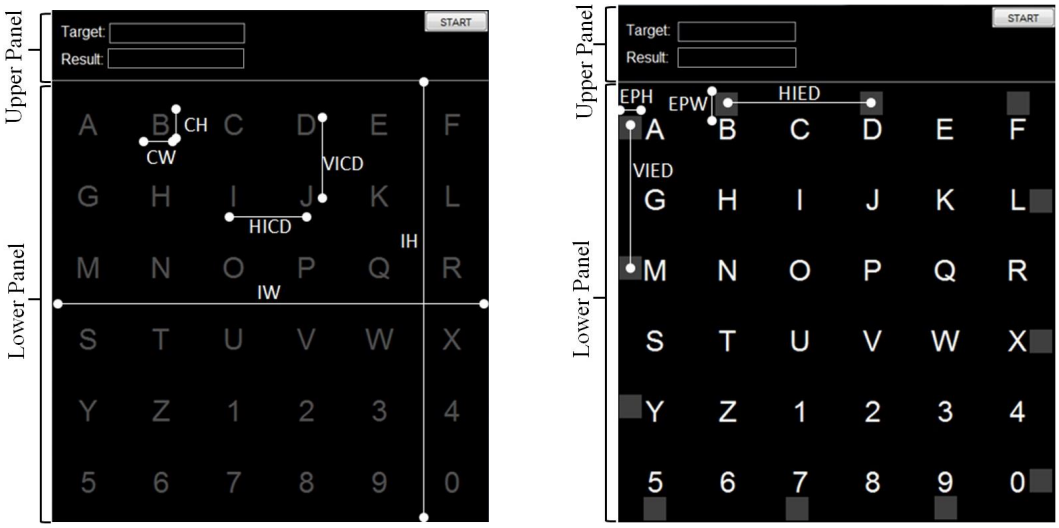

(a) (b)

Figure 17. (a) The RCP visual interface, (b) The EP visual interface.

5.1.4. Visual Stimulus Design

The visual stimulus of interest was a flash in both interfaces, as shown in Figure 18. As shown in Figure 18, when selecting a target character with the RCP, there were two stages in the randomized sequence of flash stimuli. In this sequence, there were 144 trials (flashes), with 72 row trials in the first stage followed by 72 column trials in the second stage; stages between which intervened a flash-free inter-stage interval lasting 2 seconds (s). All row and column trials were grouped into 24 blocks (12 row blocks and 12 column blocks). Each block consisted of 6 row or 6 column trials, and the same row (column) was prevented from flashing successively upon consecutive trials. Parenthetically, this investigation thus applied the flashing technique introduced by Serby *et al.* [84] to resolve the double-flash problem, which would have otherwise occurred when the target character flashed successively. In this flashing technique used in the present investigation, the column flashes began after all

Table 1. The objects' dimensions and distances between objects for the RCP and EP (cm).

Dimensions/Distances	**RCP**	**EP**
Character Height (CH)	0.68	0.68
Character Width (CW)	0.68	0.68
Edge Point Height (EPH)	—	0.68
Edge Point Width (EPW)	—	0.68
Horizontal Inter-character Distance (HICD)	2.13	2.13
Vertical Inter-character Distance (VICD)	2.13	2.13
Horizontal Inter-edge point Distance (HIED)	—	4.26
Vertical Inter-edge point Distance (VIED)	—	4.26
Interface Height (IH)	12.7	12.7
Interface Width (IW)	12.7	12.7

row flashes rather than the traditional alternation between row and column flashes, as described in [25]. The target row and column that contained the target character were evenly flashed 24 times (rarely; one time per block). The non-target row and column flashed 144 - 24 = 120 times (frequently; 5 times per block).

The EP flashing technique was exactly the same as the RCP flashing technique described above, with the exception that only the edge point was flashed rather than the entire row or column, as illustrated in Figure 19.

The stimulus-onset asynchrony (SOA) duration in both spellers (RCP and EP) was 120 ms, as consisted of 70 ms of flash and 50 ms of inter-stimulus interval (ISI). Thus, each block duration was 120 ms * 6 trials = 720 ms, and each stage lasted 720 ms * 12 blocks = 8640 ms. Overall, 2000 ms + (120 ms * 144 trials) = 19280 ms were needed to select one target character.

5.1.5. Procedure

Each participant completed an experimental session with the RCP and another experimental session with the EP. These sessions took place upon separate days.

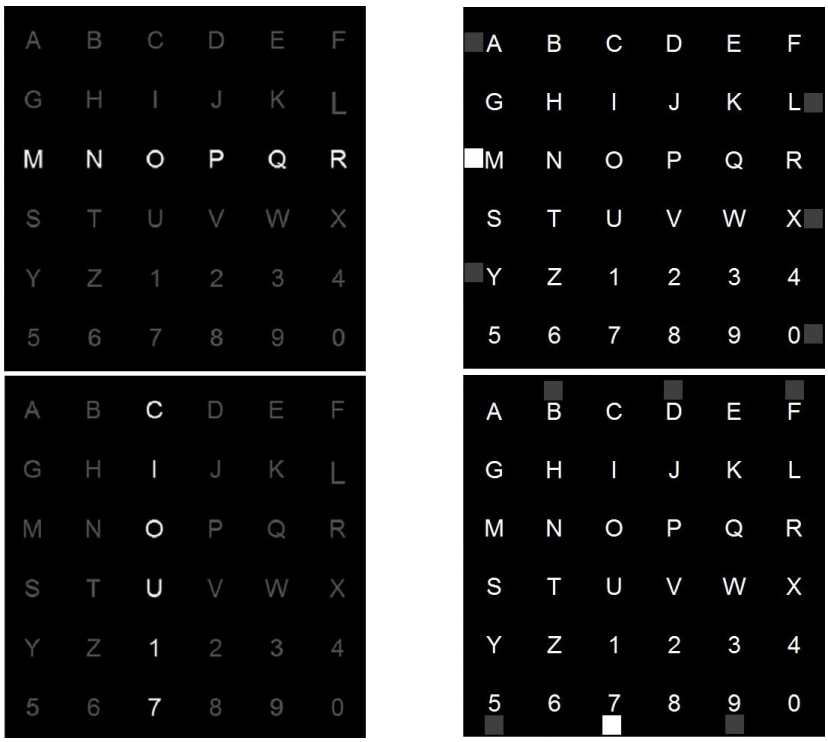

(a) (b)

Figure 18. The row and column visual flashes for the RCP (a) and EP (b).

Counterbalancing was employed such that 7 participants began with the RCP and the remaining 7 participants began with the EP. Each experiment was divided into a calibration or "offline" session, which lasted approximately 40 minutes, followed by 20 minutes for the online session. Pre-investigation and post-investigation questionnaires were filled out by the participant before and after each experiment, respectively, to rate his or her current fatigue level on a scale 1 to 10 (1: no fatigue, 10: severe fatigue). Subtraction of this pre-investigation rating from the post-investigation fatigue score was used as an index of the increase in fatigue that occurred during the task. Further, in the post-investigation questionnaire, the participant was also asked to rate his or her comfort level (1: uncomfortable, 10: comfortable) and alertness (1: drowsy, 10: alert) that he or she had felt during the experience of using the speller.

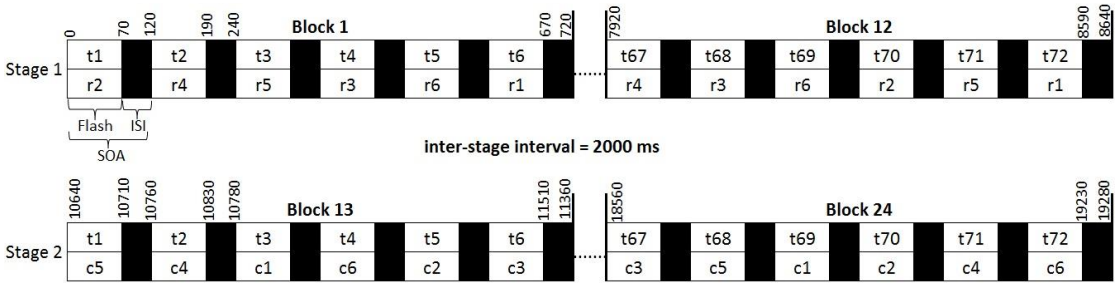

Figure 19. The flashing technique for the RCP or EP. (t: trial, r: row or row edge point, c: column or column edge point).

The participant sat on a chair in front of the speller presented on a computer screen at a distance of about 90 cm. The experimental instructions for the two spellers, RCP and EP, were different. For the RCP, participants were instructed to focus attention on a given character in the separate stages of row and column flashing. In contrast, with the EP, participants were instructed to focus attention on the edge point located on the row containing the target character in the first stage, then moving their visual focus, during the inter-stage interval, to fixate upon the edge point located on the column containing the target character in the second stage. In both spellers, participants were instructed to keep silently counting the number of times the target object (character or edge point) flashes and to minimize blinking and muscle movement during the flashing. The experiment for the current target was repeated once the participant made noticeable muscle movements, where these movements would have otherwise generated strong electric fields contaminating the electrophysiological measurements.

In the offline session for both spellers, each participant spelled 29 alphanumeric characters distributed into 6 words and a number (LAP, ROD, BAND, FLAG, DRINK, MINUTE, and 9253). The calibration data recorded in the offline session was used to train the classifier to identify the classification coefficients for each individual user (i.e., the classification model). Afterwards, in the online session, each participant

tested the classifier accuracy based on his or her classification model by spelling 16 alphanumeric characters distributed into 3 words and a number (SUM, LAMP, BUNCH, and 7492). Words and numbers were derived from the MRC psycholinguistic database [19] on the basis of having similar, relatively early, Age-Of-Acquisition norms [37].

In the offline and online sessions, the input box contained one word or a number for each run. The current target character was highlighted in red for 2 s within the matrix before the first and second stages, which allowed the participant to move his or her attention to fixate on the target object (character or edge point), and to blink and rest his or her eyes as well. In addition, specifically for the EP, a guide arrow (0.05×0.68 cm) appeared 0.09 cm above or 0.09 cm to the right of each character before the first and second stages, respectively, as illustrated in Figure 20. These arrows appeared temporarily during the highlighting, indicating the location of the edge point with the orientation of the arrow. The arrow next to the relevant character directed the participant to endogenously orient attention to fixate upon the target row or column edge point. The row edge points appeared before and during the first stage, whereas the column edge points appeared after the first stage and during the second stage.

The P300-based BCI speller framework is illustrated in Figure 21. For each single character, the Emotiv EEG signals were acquired simultaneously with the presentation of the object flashes. Then, the raw EEG data were pre-processed and recorded with a suitable format for the classifier. Finally, the application interface was used to setup communication between the classification and visual user interface to identify the target character and display it on the computer screen as feedback to the user.

(a) (b)

Figure 20. (a) The EP visual interface before 2 sec of the first stage, (b) The EP visual interface before 2 sec of the second stage.

5.1.6. Preprocessing, Feature Extraction, and Classification

The recorded EEG signals were contaminated with unwanted noises that were produced by different artefacts (eye movement, muscle and body movement, respiration, cardiac signals, and scalp skin sweating) [3, 26, 52], which could obscure the EEG signal of interest. Therefore, a digital 5^{th} order sinc filter with a bandpass of 0.16 to 45 Hz was applied by the Emotiv EEG device internally. Then, Common Average Referencing was used to increase Signal-to-Noise Ratio, which makes it easier to identify the target signal. More specifically, the average of all 14 electrodes for each time point was calculated and subtracted from all electrodes data at that time point, this process was applied on the offline and online EEG data. Then, during winsorization, the values within each offline channel data was sorted from lowest to highest values, then the 5^{th} and 95^{th} percentile amplitude values were identified channel-wise, and then that 5^{th} percentile value used to replace amplitude values falling below that 5^{th} percentile value, just as the 95^{th} percentile value was used to replace amplitudes rising above that 95^{th} percentile value in the online channel data;

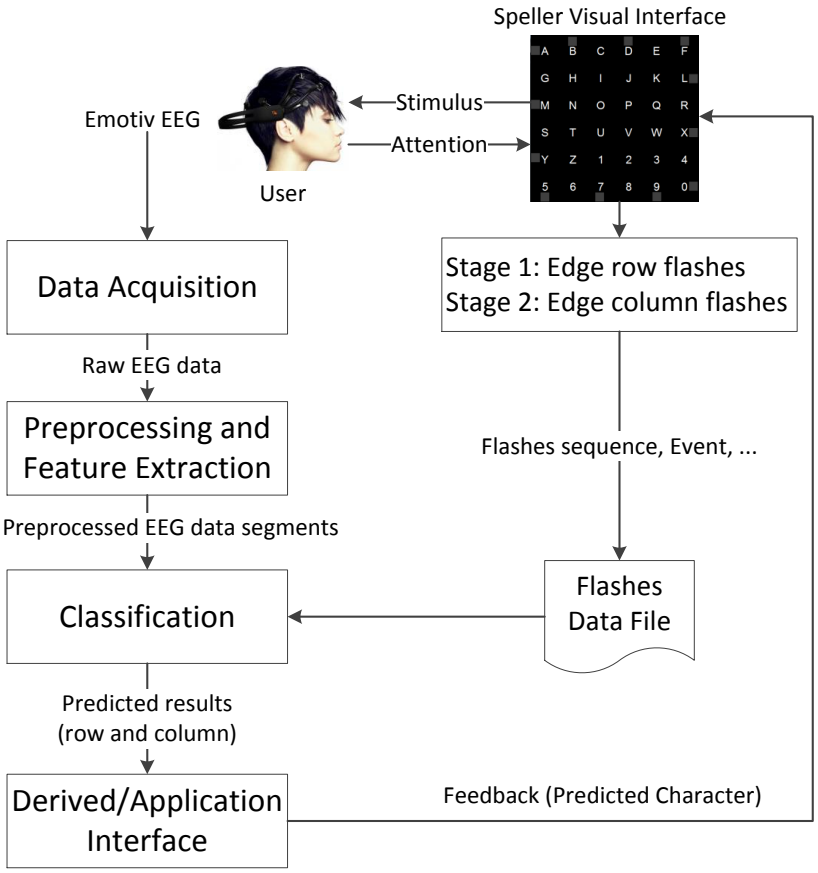

Figure 21. P300-based BCI speller framework.

effectively clipping the extremes of amplitude data during the presence of artefacts, such as eye artefact. In the normalization process, the mean and standard deviation values for each channel in the common average referenced winsorized offline EEG data were calculated, in order to normalize all channels in the online data based on z-score [46].

All pre-processed EEG data for each single target character were epoched into 600 ms sections with 144 epochs (i.e., segments), as illustrated in Figure 22. Each segment corresponded to one flash object (trial) from the stimulus onset to 600 ms post-stimulus onset (i.e., 600 ms time frame) to identify if that flash evoked the P300 component. More specifically, each segment was an individual two-dimensional matrix

structure containing EEG data recorded from 14 electrodes within 77 time points following each flash (segment size of 14-by-77), where the number of time points = ceil (0.6 s * 128 sample/s). 5% of the highest and lowest sample amplitudes (tail outliers) generated by artefacts for each electrode were reduced to the 95^{th} percentile amplitude value or increased to the 5^{th} percentile value, respectively. This process is termed Winsorizing [46].

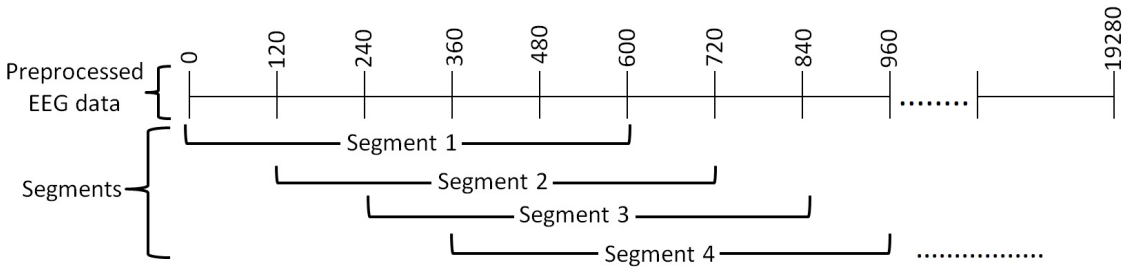

Figure 22. Feature extraction (Segmentation). The flash segment is the EEG data recorded for 600 ms after flash onset, where there are 144 flashes to select one single character with one flash every 120 ms (SOA).

Bayesian Linear Discriminant Analysis (BLDA) was implemented in this investigation to determine the target character. For each participant, the calibration EEG data of 144 * 29 = 4176 flashes (696 target and 3480 non-target flashes) were used to train the BLDA, and then the BLDA coefficients were derived. Consequently, in the online classification, BLDA was performed after the EEG data were recorded and preprocessed for each single character (144 segments) to identify the target character. The BLDA was run on all 144 segments to find the classification results for each segment. Afterwards, the BLDA-calculated values for the segments corresponding to each row (row edge point) or column (column edge point) were averaged over the 12 blocks (12 segments). The row (row edge point) or column (column edge point) with the highest average was considered as the target row and target column, respectively, as shown in Equations 5.1 to 5.4. Finally, the character located at the intersection of the target row and the target column was selected as the target character. The

identified target character was displayed in the green color for 2 s within the matrix and added to the output text box as feedback to the participant.

$$AVG\_BLDA(r_i) = (\sum_{n=1}^{12} BLDA(r_i, n))/12 \tag{5.1}$$

$$Target\_Row = max(AVG\_BLDA(r_i)) \tag{5.2}$$

$$AVG\_BLDA(c_i) = (\sum_{n=13}^{24} BLDA(c_i, n))/12 \tag{5.3}$$

$$Target\_Column = max(AVG\_BLDA(c_i)) \tag{5.4}$$

Where, a row/row edge point segment is denoted by r; a column/column edge point is denoted segment c; i signifying the row or column number (1 to 6); n the row block number (1 to 12) or the column block number (13 to 24); $BLDA(r_i, n)$ and $BLDA(c_i, n)$ representing the BLDA classification results of row i segment and column i segment respectively for block n.

5.2. Results

5.2.1. Online Character-based Classification Accuracy

As depicted in Figure 23, the pattern of the mean classification accuracy suggested that performance was improved with the EP, mean 93.3 ± standard error of the mean or s.e.m. 2.01%, relative to RCP, 81.7±2.81%. This finding was corroborated by inferential statistical analysis: a paired t-test revealed that the performance improvement produced with the EP relative to the RCP was significant, $t(13) = 4.19$, $p = 0.001$, $\eta^2 = 0.575$ (11/14 showed the effect).

The online classification performance cross 12 blocks for each participant separately and all of them together (i.e., average) as well are illustrated in Figure 24. For both EP and RCP is a strong linear tendency for an increase in character accuracy with blocks superimposed onto which is an additional tendency to asymptote (ceiling)

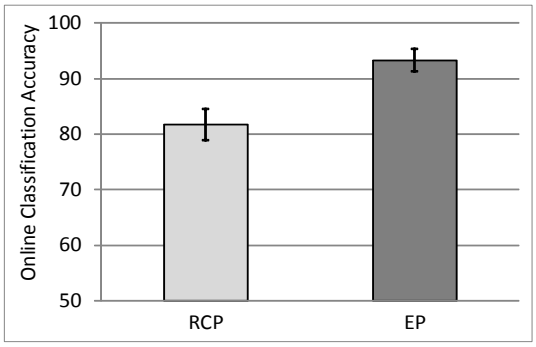

Figure 23. Mean percentage classification accuracy as a function of interface (error bars denote standard error); N=14.

tightening up the error bars toward 12 blocks. Each increment in the number of blocks initial shows a robust improvement in performance, yet not with higher numbers of blocks (this accords with the expression about signal-to-noise ratio [62]). However, a robust EP vs RCP advantage is apparent only after 8 blocks.

5.2.2. Flash Object-based Analysis of Errors

For each paradigm, the results for the 224 (16 characters * 14 participants) selected characters from the online sessions were summarized within confusion matrices of error distributions as shown in Figure 25. Given the error confusion matrix denoted by m, the number of correctly selected target characters is designated by the center cell *m(0, 0)*, as is highlighted in gray; the row '0' and column '0' representing the target row and target column, respectively. The frequency of erroneously selected characters relative to the target character is reflected by the values in the other cells. The difference in rows and columns between the erroneously selected character and the target character is signified by the cell position. If a participant selected a character with the speller, then the value of the cell position (selected row - target row, selected column - target column) within the error distribution matrix is incremented by one.

Further error analysis was computed based upon the flash objects to examine the effect of the adjacency problem in both paradigms. In Figure 25, all adjacent error

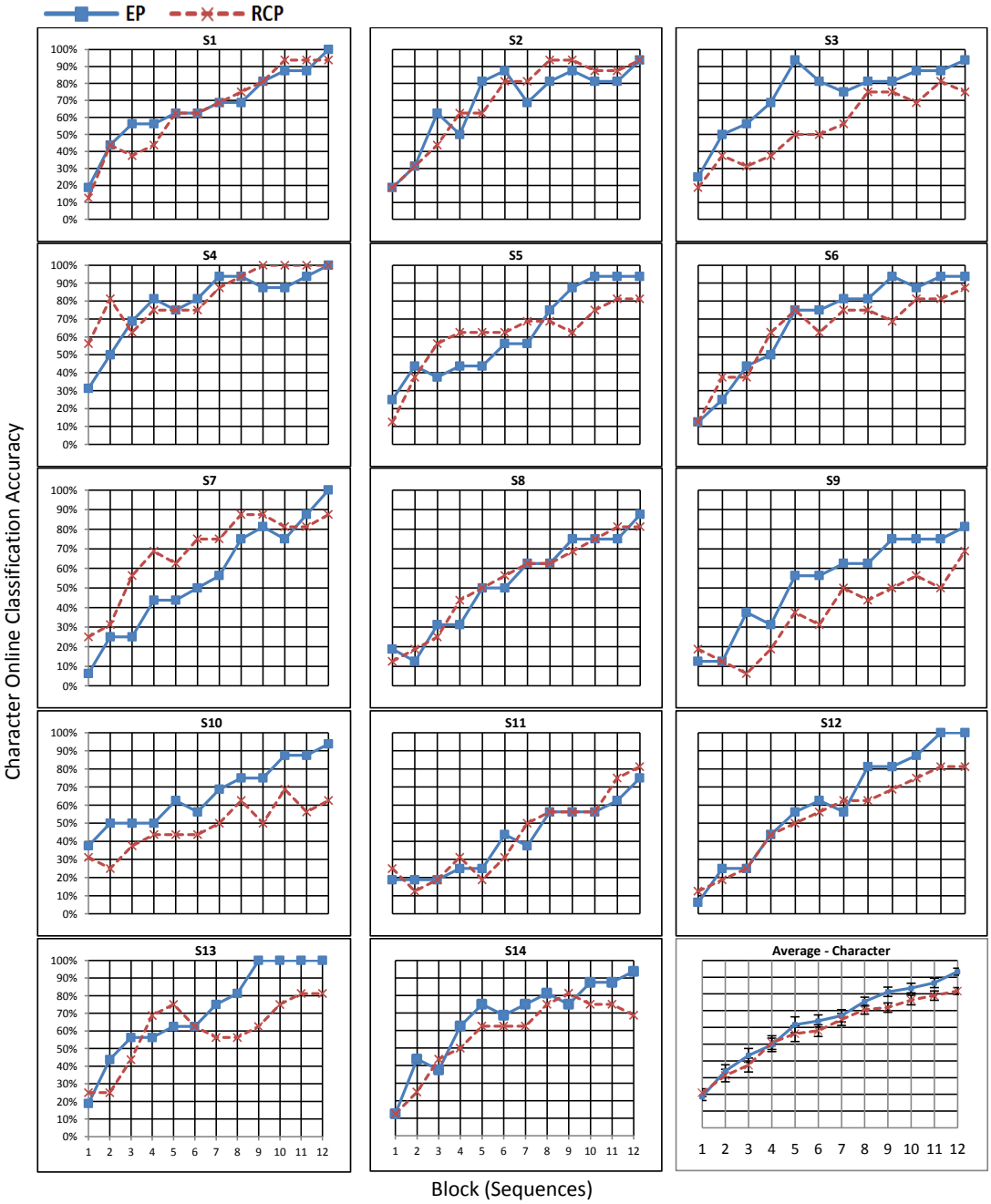

Figure 24. The online BLDA classification performance of each participant (N=14) cross blocks. The rightmost figure of the last row represents the mean classification performance cross 12 blocks for all participants

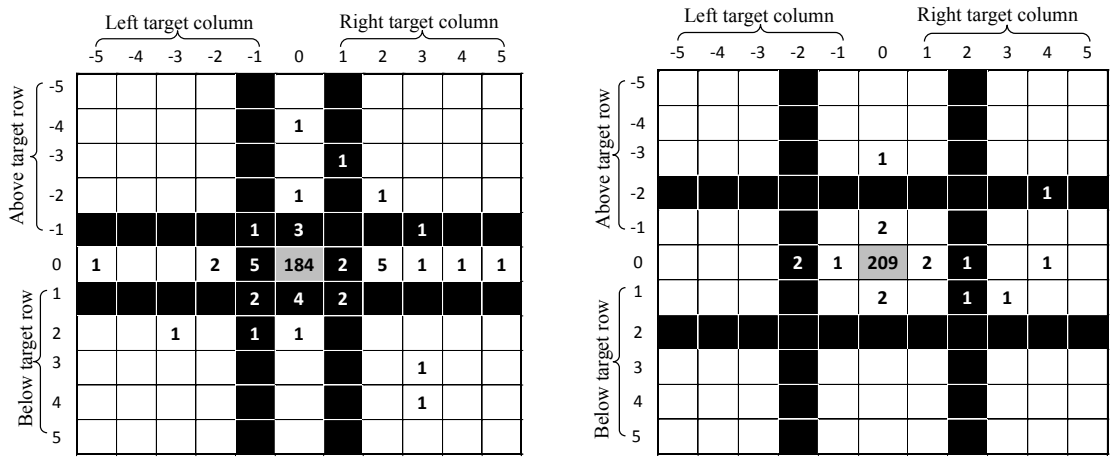

Figure 25. The error confusion matrix of all subjects for 16 selected characters in the online session for the RCP (a) and EP (b); gray cell denoting the target; black cells denoting adjacent errors, where a neighboring flash was erroneously detected as denoting the row or column of the target.

cells are highlighted in black. For the RCP, as shown in Figure 25(a), the adjacent flash rows for the target row were row '1' and row '-1', and the adjacent flash columns for the target column were column '1' and column '-1'. As depicted in Figure 25(b), the adjacency identification for the EP was different from the RCP, being based upon the edge point flash object, rather than the row or column flash in the RCP; the adjacent flash row edge points for the target row edge point were row edge point '2' and row edge point '-2', whereas the adjacent flash column edge points for the target column edge point were column edge point '2' and column edge point '-2'.

The frequencies in these confusion matrices showed that the influence of the adjacency problem was reduced with the EP. Of a total of 41 errors for the RCP, there were 28 adjacent errors (68.3%). Of a total of 15 errors for the EP, there were 5 adjacent errors (33.3%). The mean number of adjacent errors was significantly higher for the RCP, 2±0.36) than for the EP, 0.36±0.17, as was revealed to be reliable by a paired t-test, $t(13) = 4.81$, $p = 0.001$, $\eta^2 = 0.564$ (12/14 showed the effect).

5.2.3. User Experience

The user experience questionnaire data measured subjective ratings of fatigue, comfort, and alertness in both paradigms. As shown in Figure 26(a), the EP, 1.14±0.21, caused less fatigue than the RCP, 3.14±0.4. The difference of fatigue ratings before and after the experiment ranged from 0 to 9, where 0 and 9 indicated the smallest and largest fatigue caused by using the speller, respectively. Also, participants reported that EP, 8.29±0.34, was more comfortable after the experimental session relative to the RCP, 6.43±0.56, as well as more alert during the experiment of the EP, 8.5±0.39, relative to the RCP, 6.07±0.4, as shown in 26(b), where 10 indicated the highest comfort and alertness level.

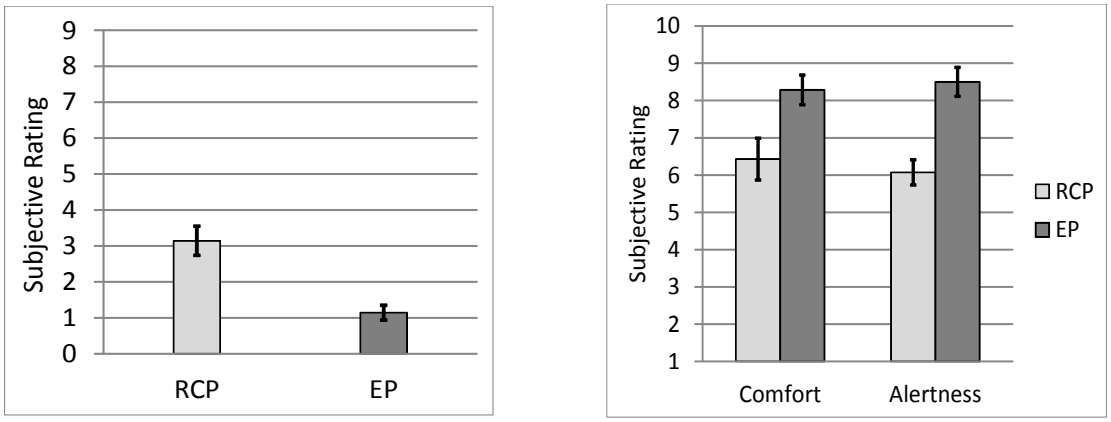

(a) (b)

Figure 26. Subjective rating for all participants (N=14). (a) Mean of the fatigue rating difference before and after the experiment (0:9). (0: lowest level of fatigue, 9: highest level of fatigue). (b) Mean of the comfort, and alertness rating (1:10). (1: lowest level of comfort and alertness, 10: highest level of comfort and alertness).

These tendencies shown in Figure 26 were broadly supported by inferential statistical analyses: paired t-tests comparing EP and RCP revealed a significant effect of interface upon fatigue, $t(13) = -5.29$, $p = 0.0001$, $\eta^2 = 0.683$ (12/14 showed the effect), comfort, $t(13) = 4.45$, $p = 0.0007$, $\eta^2 = 0.604$ (11/14 showed the effect), and upon alertness, $t(13) = 5.22$, $p = 0.0002$, $\eta^2 = 0.677$ (14/14 showed the effect).

5.3. Discussion

The results showed that the use of the EP, relative to the corresponding RCP, led to significant increases in the online classification accuracy alongside an improved user experience. That is, use of the EP caused significantly less fatigue than did the RCP, in a manner that also led to reliably enhanced levels of reported alertness and comfort. The results were thus consistent with the proposition that the design of EP ameliorated the influence of adjacent, crowding, and fatigue problems.

Concerning the adjacency problem, a large proportion of the errors with the RCP were adjacent errors as replicated the findings of previous investigations [27, 72, 90]. The number of these adjacent errors was, here, significantly reduced using the EP. The interpretation offered is that the increased spatial separation between flashes denoting neighboring characters in the EP ameliorated the influence of the adjacency problem that was more manifest for the RCP. This increased separation was attained by the relative position of the flashing squares of the EP that denoted neighboring characters by flashes upon opposite sides of the character matrix, rather than by the spatially proximal flashes of neighboring rows or columns of the RCP. There were also increased distances between adjacent flashing squares representing alternate rows or columns upon any given edge of the EP's character matrix – the increased distances of the Vertical and Horizontal Inter-edge point Distances in the EP that doubled the corresponding Inter-character Distances between the neighboring rows and columns of the RCP (Figure 17; Table 1). These increased separations led to an improvement in online classification performance, as was commensurate with an aspect of Bouma's law [12] that identification of a stimulus is improved as a function of the spatial separation between the target stimulus and flanking non-target stimuli; a law that generalized from cognitive performance to classification by P300 BCI, as further extended support for the robustness of effects of spatial separation upon online

classification performance shown previously [72].

Concerning the crowding problem, the improvement in online classification performance was also attributable to decreasing the number of similar flashed objects surrounding any target object to 1 or 2 flashed squares on each edge of the EP, instead of the 3 to 8 flashed characters in the RCP. This reduction in crowding was accomplished by reducing the number of similar neighboring flashed stimuli. That is, in the EP, there were fewer target-adjacent horizontal or vertical flashes than in the RCP and no diagonally adjacent flashes at all. Further, the flashed square representing the row or column of the target character in the EP was dissimilar to the un-flashed neighboring characters [94]. This dissimilarity is thought to have limited those characters' potency as flankers. Rather than serving as flankers, those dissimilar character objects are thought to have reduced crowding by separating that attended edge square from the other to-be-ignored edge points upon the opposite side of the matrix. That this square denoting the target row or column was attended [92] in central fixation – when according to Bouma's law [12], crowding increases with target eccentricity – is also thought to have reduced any crowding produced by neighboring squares on the same edge.

The fatigue problem was also ameliorated by EP as demonstrated by the ratings of user experience, which revealed that the EP caused reliably less fatigue than use of the corresponding RCP. Additional consistent outcomes were that after using the EP interface, participants rated themselves as feeling significantly more alert and comfortable than they did after using the corresponding RCP. Taken together, the results have offered support for the conclusion that EP has addressed the fatigue problem by virtue of reducing the influence of the crowding and adjacency problems on the neurocognitive processes that determined P300 generation, which, in turn, increased online classification performance.

The EP can be implemented using devices with smaller displays; devices less suited to resolutions of the adjacency and crowding problems that have necessitated increased separation between characters [72] that, in turn, would require expansion of these dimensions beyond the limits of the device's screen size. Such mobile devices considered include commercially available tablet PCs and, as RAM and processor speeds increase, smartphones. That is, here, the EP interface subtended a visual angle of 8 degrees in height and width here, as would fit well within a 5 x 5 cm display at a comfortable viewing distance of 35 cm upon a mobile device that could be mounted on a wheelchair. Such a small device is considered particularly applicable for many BCI applications, only occupying a large proportion of the field-of-view when attended, such that the user could safely navigate and interact with his or her environment without visual obstruction. That is, envisaged is that P300 BCI on such a mobile device could be used to access information and communication technologies, including the control of text-to-speech synthesis for speech communication, and the motors of a wheelchair such that the user can navigate the world leading a productive and fulfilling life in relative independence.

CHAPTER 6. COMPARATIVE STUDY: RCP VS ZP VS EP

The online classification performance and user experience for the P300 speller were significantly improved with the Zigzag Paradigm (ZP) and Edges Paradigm (EP) relative to the Row-Column Paradigm (RCP). The ZP and EP improvements were investigated in two separate studies explained in Chapter 4 and 5, respectively. These improvements were achieved by reducing the effect of the RCP problems, such as crowding, adjacent, and fatigue problems. Particularly, the EP made further physical interface and stimulus improvements on the RCP than the ZP.

The distance between all adjacent flashed objects (i.e., edge points) was doubled in the EP, while shifting the even rows in the matrix little increased the distance between most adjacent flashed objects (i.e., characters). Furthermore, the EP reduced the number of flashed objects surrounding any object, *flankers*, relative to the ZP. This chapter explores how the influence of the physical crowding and adjacent levels in the P300 speller interface can affect its performance and user experience using the RCP, ZP, and EP. In addition, Section 6.3 shows how a reduction in crowding could improve speller classification.

6.1. Methods and Materials

6.1.1. Participants

18 neurologically normal able-bodied participants (15 male; age 20-35 years; mean: 27.7 years; S.D.: 4.45) were voluntarily involved in a user study. The user study was approved by the North Dakota State University Institutional Review Board, in accordance with the Declaration of Helsinki. All gave their informed written consent prior to their participation in the experiment.

All hardware, software, toolboxes, and materials listed in Chapter 3, Section 3.1.2., were used in this study.

6.1.2. Visual Interfaces Design

As explained in Section 4.1.3 and 5.1.3, the RCP, ZP, and EP interfaces were divided into a smaller upper part and a larger lower part. The small top was identical in the three interfaces and consisted of a command button used to run the speller, input text box to display a target text, and output text box to display the user's selection text (one character at a time). In contrast, the large lower part was different for the three interfaces. In the RCP, the lower part included a 6-by-6 matrix with 36 gray alphanumeric characters (see Figure 27(a)). In the ZP, every second row of the RCP matrix is offset to the right by *HICD*/2 cm, where *HICD*, 2.13 cm, is the horizontal inter-character distance (see Figure 27(b)). In the EP, the color of the RCP matrix characters was changed to white instead of gray, also, a gray edge point is added to the left side of every odd row, right side of each even row, below every odd column, and above each even column of the RCP matrix (see Figure 27(c)).

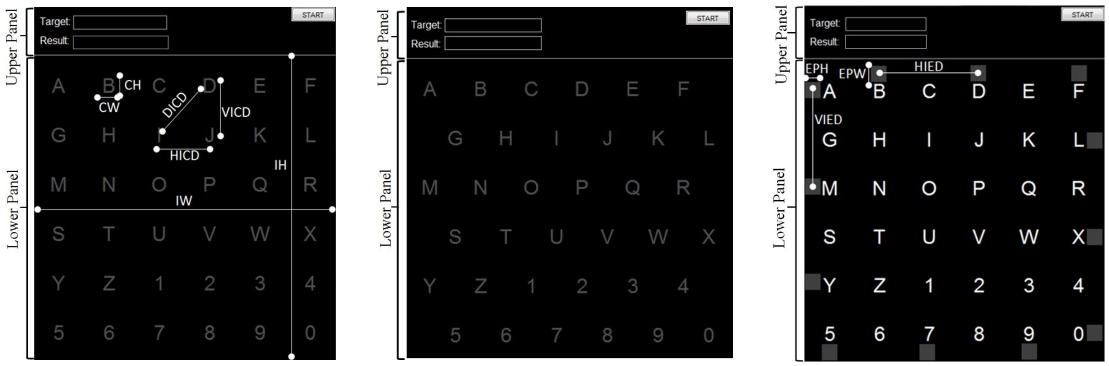

(a) (b) (c)

Figure 27. Visual P300 speller interface for: (a) RCP, (b) ZP, and (c) EP.

Regarding the crowding problem, the shifting process in the ZP reduced the number of similar shape flashed characters surrounding any character from 3, 5, or 8 characters in the RCP to 2, 5, or 6 characters in the ZP. The crowding problem was reduced significantly by the EP, whereas each flashed edge point was surrounded by 1 or 2 edge points.

As shown in Figure 27, the distance between most adjacent flashed characters in the ZP was increased relative to the RCP, while the distance between adjacent flashed edges points in the EP was doubled. All interfaces dimensions and distances between objects are elaborated in Table 2.

Table 2. The objects' dimensions and distances between objects for the RCP, ZP, and EP (cm).

Dimensions/Distances	**RCP**	**ZP**	**EP**
Character Height (CH)	0.68	0.68	0.68
Character Width (CW)	0.68	0.68	0.68
Edge Point Height (EPH)	—	—	0.68
Edge Point Width (EPW)	—	—	0.68
Horizontal Inter-character Distance (HICD)	2.13	2.13	2.13
Vertical Inter-character Distance (VICD)	2.13	—	2.13
Horizontal Inter-edge point Distance (HIED)	—	—	4.26
Diagonal Inter-character Distance (DICD)	3.01	2.38	3.01
Vertical Inter-edge point Distance (VIED)	—	—	4.26
Interface Height (IH)	12.7	12.7	12.7
Interface Width (IW)	12.7	13.765	12.7

6.1.3. Visual Stimulus Design

Visual stimuli were *flashes* denoting characters, as shown in Figure 28. In this figure, the RCP or ZP required 144 row and column flashes (trials) to select one target character. All rows were flashed 72 times in stage 1 followed by 72 column flashes in stage 2, with a 2 s inter-stage interval when no flash was presented. The trials of each stage were grouped into 12 blocks, and each block contained 6 trials (1 target and 5 non-target trials). In a row block of six random flashes, one flash denoted each of the six rows; in column blocks, flashes denoted columns. Within blocks, the order of rows or columns quasi-randomized such that no row or column was flashed successively

precluding the double-flash problem [84]. The SOA duration was 120 ms (70 ms of flash and 50 ms of ISI). Thus, one target character selection lasted 19.28 s (144 trials * 0.120 s + 2 s inter-stage interval).

In the EP, the flashing technique was exactly the same as RCP and ZP flashing technique, but the row or column edge point was flashed instead of the corresponding row or column.

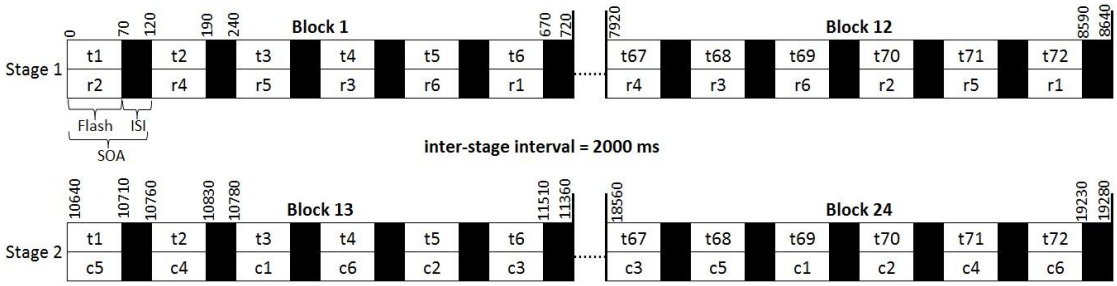

Figure 28. Row flashes (stage 1) and column flashes (stage 2) for each target character in the RCP, ZP, and EP. (t: trial, r: row or row edge point, c: column or column edge point).

6.1.4. Procedure

During all experimental sessions, the speller interface was presented at a viewing distance of 90 cm. Each subject used one of the BCI spellers for two sessions during upon one of three experiments on separate days, such that each participant completed two sessions using each speller. The order of assignment of the speller to these experiments was counter-balanced across subjects. The first BCI session of an experiment was an offline session during which the subject was instructed to copy-spell characters from alphanumeric strings presented letter-by-letter one-at-a-time above the interface (LAP, ROD, BAND, FLAG, DRINK, MINUTE, 9253); a session from which the scalp-recorded data and flash sequences were used to train the classifier. In the subsequent online session, the trained classifier was tested using16 characters (SUM, LAMP, BUNCH, and 7492) while electrophysiological recordings were also made. Words were drawn from the MRC psycholinguistic database with

similar, relatively early, Age-Of-Acquisition norms [37].

Instructions for the use of the relevant speller were explained to each participant before starting the relevant experiment. For both offline and online sessions, instructions for RCP and ZP use specified to fixate upon the target character and to count the number of target character flashes in each stage. The instructions for EP use stated instead to fixate the target row edge point, located on the target character row edge, in stage 1, and then to reorient fixation toward the target column edge point, located on the target character column edge, in stage 2. This reorientation from rows to columns or the corresponding edge squares took place during the inter-stage interval. In the online session, the character predicted by the classifier was colored green providing feedback in real-time.

Directly before and after each experiment, each subject rated current level of fatigue upon a 10-point Likert item (1: no fatigue, 10: severe fatigue). Directly after each experiment, each subject similarly rated levels of comfort (1: uncomfortable, 10: comfortable), and alertness (1: drowsy, 10: alert). The participants rating were analyzed statistically to know the effect of each speller interface on the user experience. The EEG data acquisition procedure is illustrated in Figure 29 (left panel), and the fully detailed procedure was explained in Section 4.1.5 and 5.1.5.

6.1.5. Preprocessing, Feature Extraction, and Classification

For each paradigm separately, for each individual's data, the offline and online recordings underwent a preprocessing consisting of Filtering, Common Average Referencing, winsorizing [46], and normalization steps intended to reduce the influence of any artefacts obscuring the EEG signal, in order to increase Signal-to-Noise Ratio (SNR), as shown in Figure 29. Thus, most of the contaminated and unnecessary data (noise) were eliminated from the raw EEG data to make it more useful. Data recorded when the flashes denoting rows underwent this preprocessing separately from

data recorded when the flashes denoting columns.

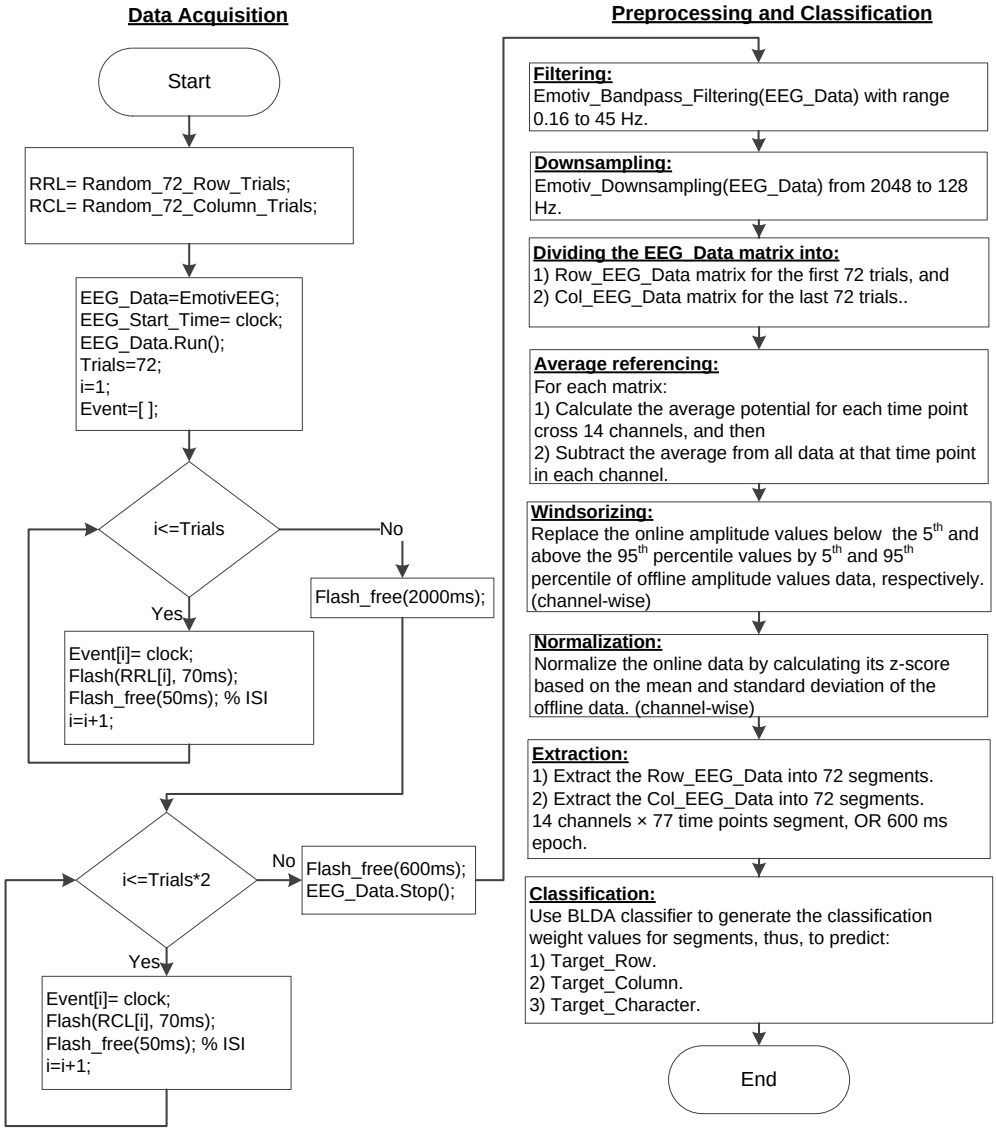

Figure 29. Data acquisition, preprocessing, and classification procedure.

During each experiment, the Emotiv EEG wireless headset, Research Edition, digitised signals at 128 Hz within a bandpass of 0.16 to 45 Hz (5^{th} order sinc filter). All preprocessing steps, such as Common Average Referencing, winsorizing, and normalizing were explained in Section 5.1.6.

All pre-processed EEG data for each target character were epoched into 600 ms sections with 144 epochs (i.e., segments), as mentioned in Section 5.1.6 and illustrated in Figure 22.

Pooled EEG date segments, online and offline EEG data, were sorted into bins according to whether the stimulus was a row or a column; these rows and column bins being divided into bins where the flash was a target or a non-target. In later analyses, these non-target bins were further subdivided into bins according to whether the non-target flash was a flanker or non-flanker. However, whether the non-target was a flanker or a non-flanker was not used for classification.

Rather, the Bayesian Linear Discriminant Analysis (BLDA) classification algorithm [65] was trained to differentiate the EEG features corresponding to a target or a non-target. Separately with offline epochs in bins where the flash denoted a row, and separately with offline epochs from bins where the flash denoted a column, the BLDA was trained with the pre-processed epoched data to define classification statistical attributes. These attributes were used to calculate a classification weight value for each testing segment, this value called class label, which is between 0 and 1and indicate how probability of segment to be the target. Lastly, the highest average of all probabilities values for all segments corresponding to each row or column across 12 blocks consider as the target row and column, respectively, and the intersection character between target row and column is the target character [46]. The classification process is fully explained in Section 5.1.6.

6.2. Results

For each subject and paradigm, the online classification accuracy was the percentage of the number of characters, presented to copy-spelled on the online session, which were selected correctly by the appropriately trained BLDA. Similarly, for each subject and paradigm, the corresponding fatigue score was computed by subtracting

the reported level of fatigue before the experiment from that reported after the experiment. Other user experience measures were those in the for comfort and alertness Likert items. Accordingly, the approach to hypothesis testing was *priori*, considering an overall effect of interface determined by 1-way repeated-measures Analysis of Variance (ANOVA) with "interface" (RCP, ZP, EP) as the independent variable and online classification performance or each user experience as dependent variables, together with linear contrasts comparing RCP to ZP and ZP to EP levels of interface.

6.2.1. Online Character-Based Classification Accuracy

As depicted in Figure 30, mean online classification performance according to the notion that these new interfaces effectively address the crowding problem, particularly, the EP (RCP: mean 80.21±s.e.m. 2.33% < ZP: 87.50±1.96% < EP: 93.75±1.13%).

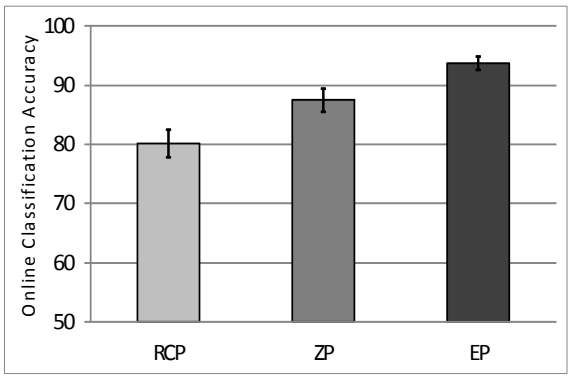

Figure 30. Mean percentage classification accuracy as a function of interface (error bars denote standard error); N=18.

A 1-way repeated-measures ANOVA (interface: RCP, ZP, EP) upon online classification performance confirmed a highly significant main effect of interface, $F(2, 34) = 24.82$, $p = 0.0000002$, $\eta_p^2 = 0.593$, replicating the previously demonstrated advantage of ZP over RCP [72] and EP over RCP. Planned linear contrasts corroborated this interface effect was not only due to a highly significant performance advantage shown with the ZP over RCP, $F(1, 17) = 11.41$, $p = 0.004$, $\eta^2 = 0.402$

(11/18 showed the effect), but also a further highly significant performance advantage of EP over ZP, $F(1, 17) = 15.30$, $p = 0.001$, $\eta^2 = 0.474$ (14/18 showed the effect); an original result of practical importance.

6.2.2. Flash Object-Based Analysis of Errors

For each paradigm, 18 participants selected 288 characters (18 participants * 16 online characters) in the online session. These selection results were presented within error confusion matrices (m) as shown in Figure 31. The center cell $m(0, 0)$, highlighted in gray, contained the number of target characters selected correctly. The other cells contained the number of characters selected incorrectly relative to the target character. For example, if the target character 'U', which is located on the row 4 and column 3 in a speller interface, was selected correctly, then the value in cell $m(0,0)$ is incremented by 1; otherwise, if the target character 'U' was selected incorrectly by 'J', which is located on row 2 and column 4, then the value in cell m(selected row - target row, selected column - target column) = $m(-2, 1)$ is incremented by 1.

The error confusion matrix does not reflect the numbers of correct and incorrect target characters selection only, but it also shows the effect of the adjacency and crowding problems upon flashed objects for each paradigm. The flashed objects in the RCP and ZP are rows and columns, while it is the edge points in the EP. In Figure 31, all adjacent error cells are highlighted in black. In the RCP and ZP, as shown in Figure 31(a) and Figure 31(b), the rows '1' and '-1' were the horizontal adjacent rows for the target row '0', and column '1' and '-1' were the vertical adjacent columns for the target column '0'. In the EP, as depicted in Figure 6.2.2, the row edge points '2' and '-2' were the horizontal adjacent row edge points for the target row edge point, whereas the column edge points '2' and '-2' were the vertical adjacent column edge points for the target column edge point.

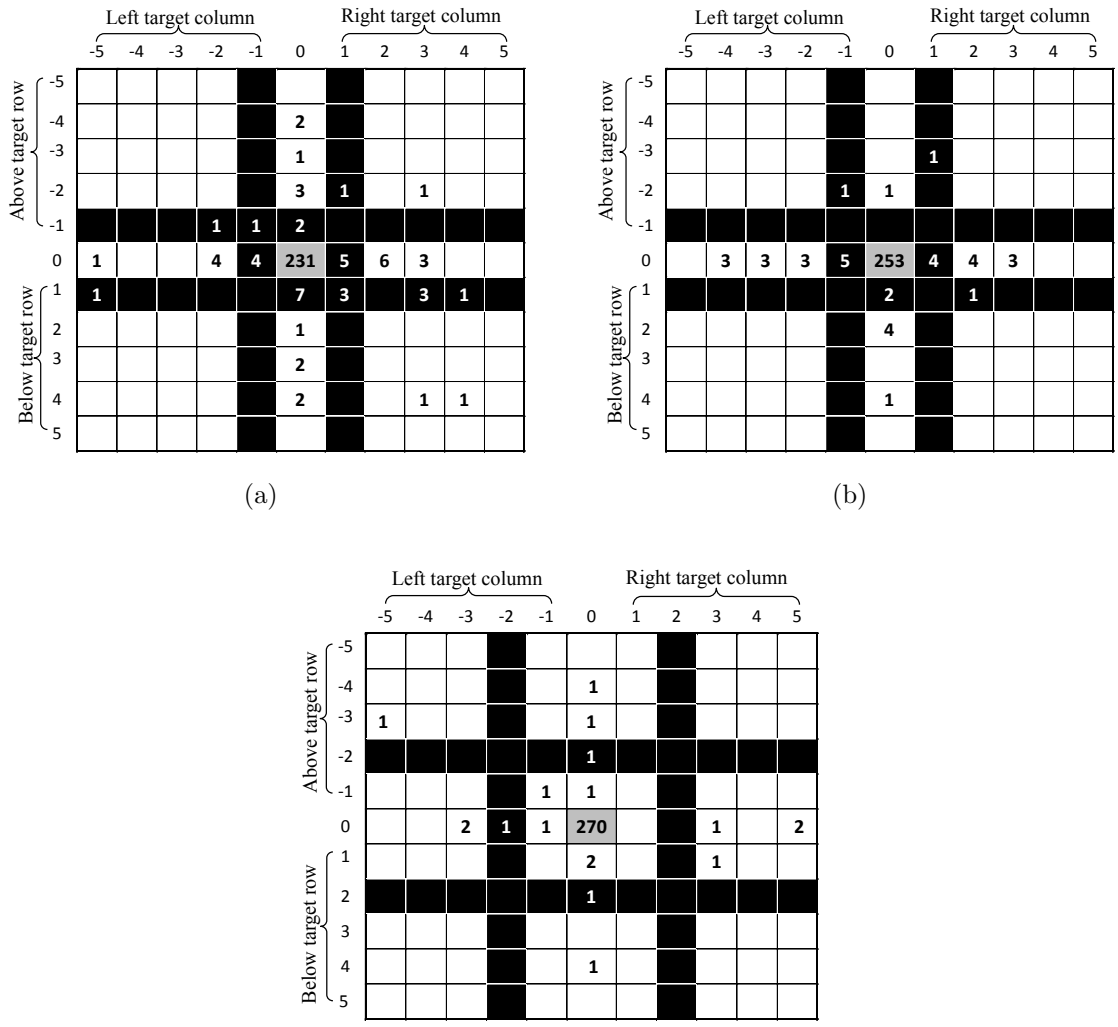

Figure 31. The error confusion matrix of all subjects for 16 selected characters in the online session for the RCP (a), ZP (b), and EP (c); gray cell denoting the target; black cells denoting adjacent flashed object errors, where a neighboring flash was erroneously detected as denoting the row or column of the target.

For each selected character, the BLDA classifier was implemented two times to predict the target row and target column independently, then further adjacent error analysis was computed based on row (or row edge point) adjacent error (horizontal) and column (or column edge point) adjacent error (vertical).

The mean±s.e.m. of the horizontal adjacent errors was larger in the RCP relative the ZP and EP (RCP: 1.056±0.171 > ZP: 0.167±0.090 > EP: 0.111±0.076). These findings were corroborated by inferential statistical analysis: A 1-way repeated-measures ANOVA (interface: RCP, ZP, EP) upon horizontal errors confirmed a highly significant advantage shown with the ZP over RCP, $F(1, 17) = 24.73$, $P = 0.0001$, $\eta^2 = 0.593$ (13/18 showed the effect), but there is no significant between ZP and EP, $F(1, 17) < 1$, $P > 0.05$, $\eta^2 = 0.011$.

The mean±s.e.m. of the vertical adjacent errors was larger in the RCP relative the ZP and EP (RCP: 0.778±0.173 > ZP: 0.611±0.165 > EP: 0.056±0.056). In a 1-way repeated-measures ANOVA (interface: RCP, ZP, EP) upon vertical errors found no significant advantage shown with the ZP over RCP, $F(1, 17) < 1$, $P > 0.05$, $\eta^2 = 0.029$, but there is a highly significant advantage shown with the EP over ZP, $F(1, 17) = 9.043$, $P = 0.008$, $\eta^2 = 0.347$ (9/18 showed the effect).

6.2.3. User Experience

These online classification performance findings were also reflected by the user experience variables, as depicted in Figure 32. As depicted in Figure 32(a), the difference fatigue levels in the three spellers were as following: (RCP: 3.83±0.38 > ZP: 2.44±0.33 > EP: 1.56 ±0.27). In addition, as depicted Figure 32(b), comfort (RCP: 5.78±0.42 < ZP: 7.17±0.33 < EP: 8.33±0.37) and alertness (RCP: 6.00±0.50 < ZP: 7.17±0.36 < EP: 8.61±0.22). The online classification performance consistent with the view that the crowding problem causes the fatigue problem experienced by users of BCI spellers.

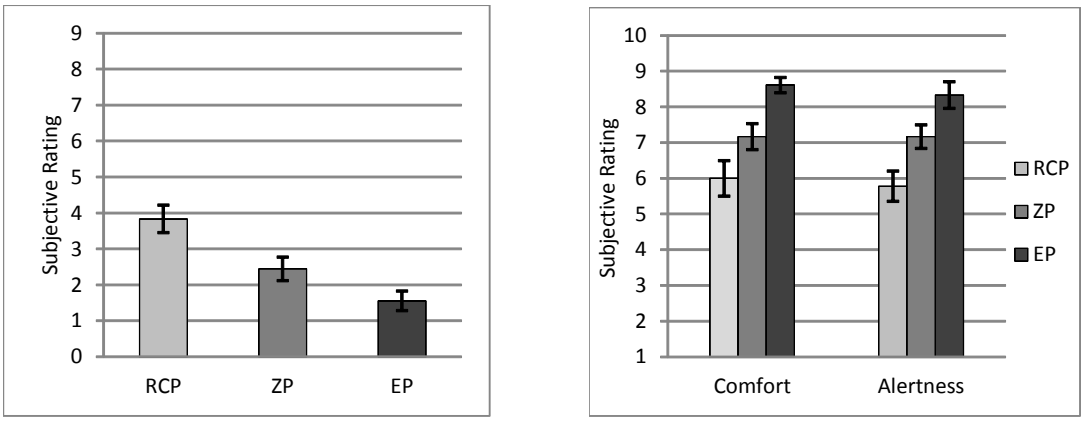

(a) (b)

Figure 32. Subjective rating for all participants (N=18). (a) Mean of the fatigue rating difference before and after the experiment (0:9). (0: lowest level of fatigue, 9: highest level of fatigue). (b) Mean of the comfort, and alertness rating (1:10). (1: lowest level of comfort and alertness, 10: highest level of comfort and alertness).

An analogous ANOVA showed that there was a highly significant main effect of interface on increases in subjectively reported levels of fatigue from before until after the experiment, $F(2, 34) = 18.66$, $p = 0.00007$, $\eta_p^2 = 0.523$, $\epsilon = 0.69$, which was not only due to the ZP causing less fatigue than the RCP, $F(1, 17) = 36.26$ (17/18 showed the effect), $p = 0.00001$, $\eta^2 = 0.681$, but also the EP causing significantly less fatigue than the ZP, $F(1, 17) = 5.06$, $p = 0.038$, $\eta^2 = 0.229$ (13/18 showed the effect).

An ANOVA upon subjective ratings of comfort level made after using the device similarly showed a highly significant main effect of interface, $F(2, 34) = 21.93$, $p = 0.000004$, $\eta_p^2 = 0.563$, caused not only by ZP use being more comfortable than RCP use, $F(1, 17) = 11.41$, $p = 0.004$, $\eta^2 = 0.402$ (13/18 showed the effect), but also EP use being much more comfortable than ZP use, $F(1, 17) = 18.54$, $p = 0.0005$, $\eta^2 = 0.522$ (15/18 showed the effect).

An ANOVA upon subjective ratings of alertness made just after device use also revealed a highly significant main effect of interface, $F(2, 34) = 17.76$, $p = 0.0001$,

$\eta^2 = 0.511$, $\epsilon = 0.66$, caused not only by users being significantly more alert after using the ZP than after using the RCP, $F(1, 17) = 15.42$, $p = 0.001$, $\eta^2 = 0.476$ (14/18 showed the effect), but also by a highly significant alertness advantage of EP over ZP, $F(1, 17) = 12.07$, $p = 0.001$, $\eta^2 = 0.415$ (13/18 showed the effect).

6.3. Discussion

The results showed that the speller online classification performance and the user experience were significantly improved from RCP to ZP to EP, upon the 1-way repeated-measures ANOVA. These results emphases the results of the previous two studies explained in Section 4.2 and 5.2.

Furthermore, the numbers of incorrect horizontal and vertical adjacent selection upon flashed objects were larger in the RCP relative to ZP, and in the ZP relative to EP. Also, ANOVA showed that the number of the horizontal adjacent errors in the RCP was significantly higher than the ZP; even higher for the ZP than the EP. In contrast, ANOVA did not show significance between the number of vertical errors between RCP and ZP, but the number of vertical errors in the ZP was significantly higher than the EP.

While researchers have shown non-targets surrounding those targets, flankers, hinder the speller's classification [27, 90], and that flankers can hamper perceptual identification of a parafoveal target [12, 94], it was previously not understood how that crowding takes place. Particularly, the large effects [18] of interface on performance and user experience indicated that the available features of the EEG information better reflected target identity for the ZP than for the RCP; even better for the EP than the ZP. According to neurocognitive principles common to the majority of users, different paradigms could engage different flanker-sensitive and target-selective processes as defined below.

Of theoretical interest was whether additional brain processes responsive to

the stimulus being a target, flanking, or non-flanking a target would add to the global power ERPs (potential average of all electrodes). 77 replicates of paired-samples permutation t-tests [38] were calculated for each global power sampling point between the start of stimulus presentation, 600 ms after stimulus onset, for the following pairs of experimental conditions of a priori interest for each of the three paradigms: "target" vs "flanker" (target-selective comparison), "flanker" vs "non-flanker" (flanker-sensitive comparison). P-values for all 462 tests (77 global power * 2 experimental conditions * 3 paradigms) were adjusted for multiple comparisons [7].

Taken to reveal the action of additional or more vigorously generated brain processes, windows of flanker-sensitive significantly increases in global power depicted in Figure 33 are evident for the RCP and EP, yet not with the ZP. Further, only ZP targets showed windows of target-selective global power increases with significantly discernible scalp distributions. Underneath each global power function, are the sample-wise time-course of the adjusted P-values [7] from permutation-based paired t-tests [38] for the theoretically relevant comparisons. Flanker-sensitive comparisons were those of non-flanker to flanker; target-selective, flanker to target. Significant P-values were those under a critical alpha α of 0.05, as represented when p-values, plotted upon a reversed logarithmic scale above the magenta line representing this significance threshold. Shaded areas represent windows of consecutive significant differences.

On the whole, RCP exhibited flanker-sensitive effects, including an early P300 effect (188-195 ms, Figure 34), thought to cause crowding without target-selective effects. For an extensive characterization of the ERPs corroborative of this flanker-sensitivity of RCP without target-selectivity, and discussion of the P300 latency, please see Supplementary Notes. ZP succeeded in overcoming crowding, exhibiting target-selective processes, the earliest of which – a target-selective early selective

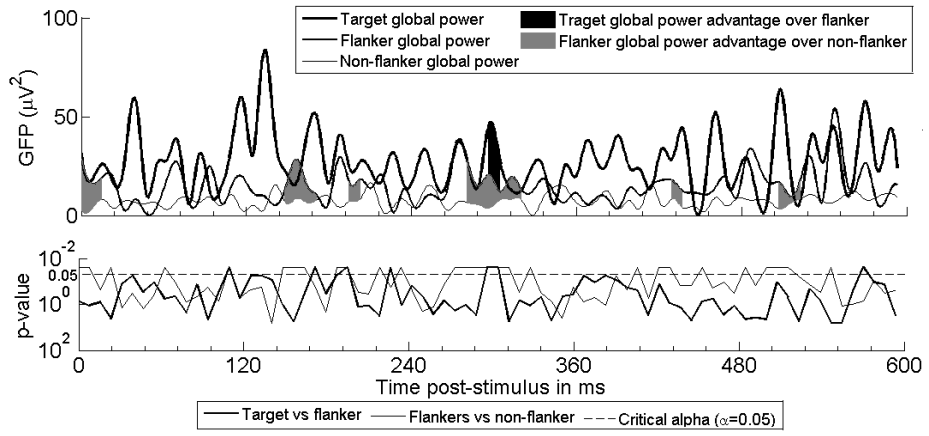

(a)

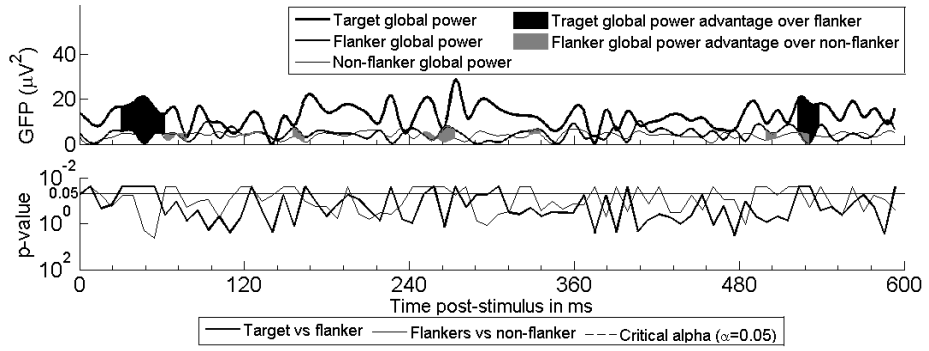

(b)

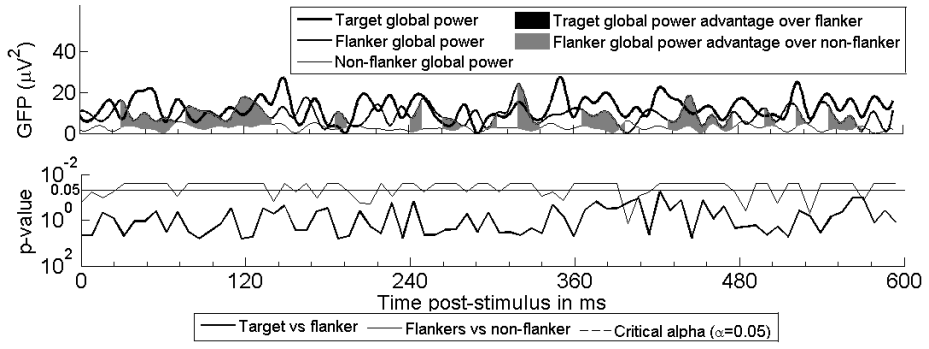

(c)

Figure 33. The ERP amplitudes averaged across electrodes, global power, as a function of target condition for a) RCP, b) ZP, and c) EP.

attention effect, a parietal positivity at 31-55 ms (Figure 35) – is thought to have prevented further flanker-sensitive processes. A P300 effect at 523-531 ms is thought to have further processed the target.

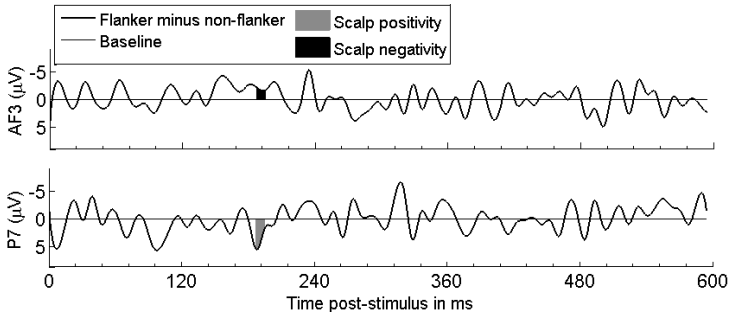

(a)

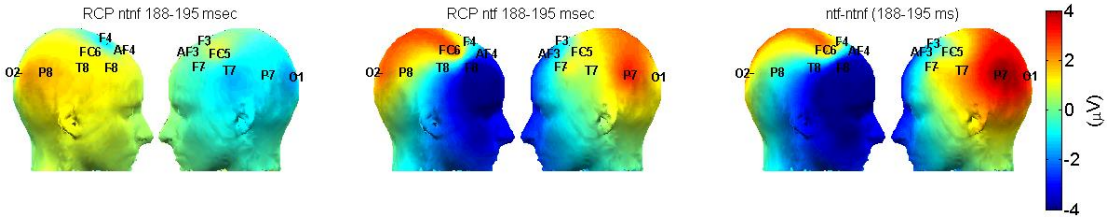

(b)

Figure 34. Flanker-sensitive comparison function at selected electrodes in the RCP. (a) difference waves with highlighting significant differences, (b) isopotential maps. (ntf: non-target flanker; ntnf: nontarget non-flanker).

EP neither exhibited these target-selective processes shown by the ZP, nor the flanker-sensitive processes shown with the RCP, but rather is thought to have been even more successful by eliciting different flanker-sensitive suppressive processes operating in different time ranges: Crucially, a temporally distributed suppression negativity at 180-188 ms (Figure 36) suppressed the subsequent processing of EP flankers that was otherwise shown to occur during the early P300 processing of the RCP flanker (188-195 ms, Figure 35). With the EP, there was further suppression frontocentral negativity at 359-391 ms and suppression frontocentral positivity at 539-563ms (Figure 36), which differed in topography from the target-sensitive P300 shown with the ZP (Figure 35).

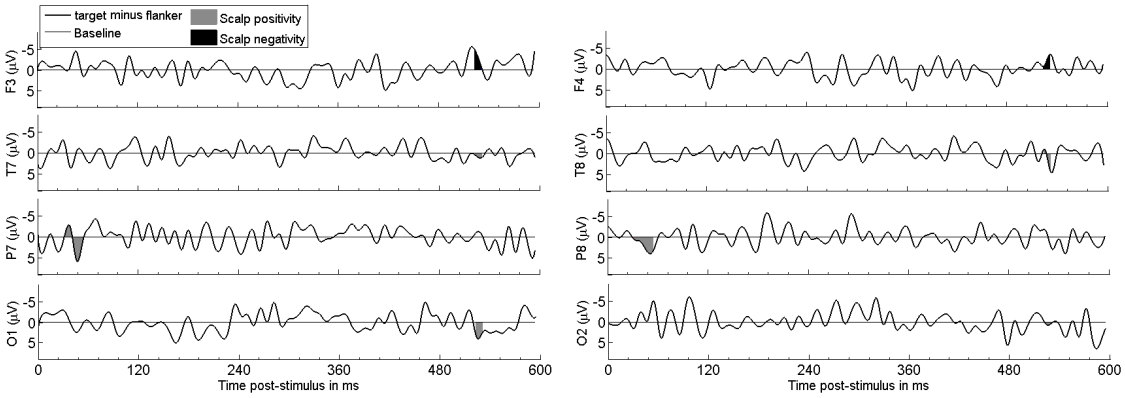

(a)

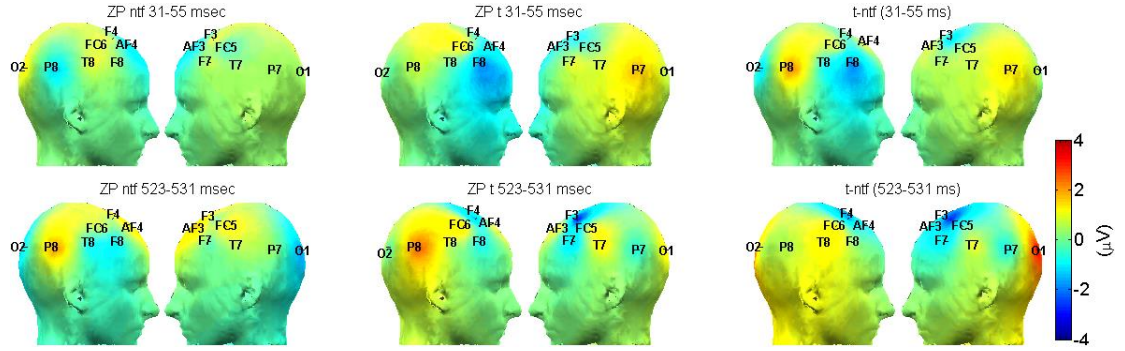

(b)

Figure 35. Target-selective comparison function at selected electrodes in the ZP. (a) difference waves with highlighting significant differences, (b) isopotential maps. (t: target; ntf: non-target flanker).

A temporally distributed N2 effect [32] (180-188 ms) at T7 and T8: $F(1,17) = 4.57$, $p = 0.047$, $\eta_p^2 = 0.212$, over the isopotential map's temples, a frontocentral negativity (359-391 ms), $F(1,17) = 10.03$, $p = 0.006$, $\eta_p^2 = 0.371$ – which is left-lateralised, $F(1,17) = 4.84$, $p = 0.042$, $\eta_p^2 = 0.222$, and reversed at frontal sites, $F(1,17) = 5.87$, $p = 0.027$, $\eta_p^2 = 0.257$ – together with a late frontocentral positivity (539-563 ms), $F(1,17) = 4.69$, $p = 0.045$, $\eta_p^2 = 0.216$.

Alongside performance and user experience measures, for a given user, these flanker-sensitive ERP effects for the EP, or in their absence, the target-selective effects for the ZP, are viable indicators of neurologically normal generator processes

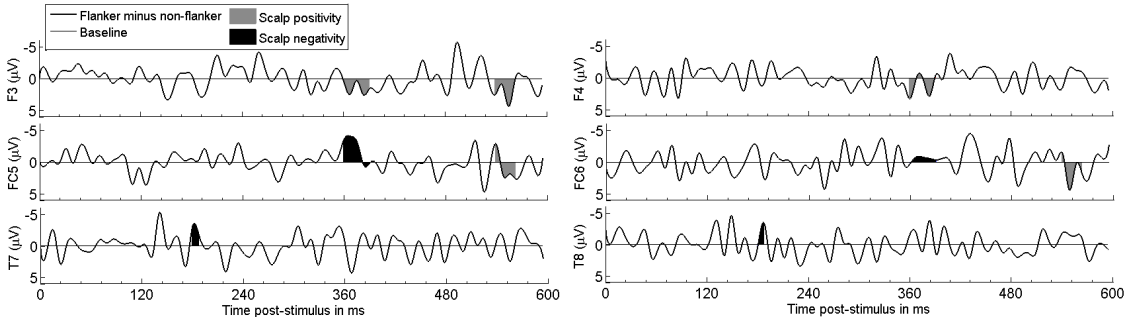

(a)

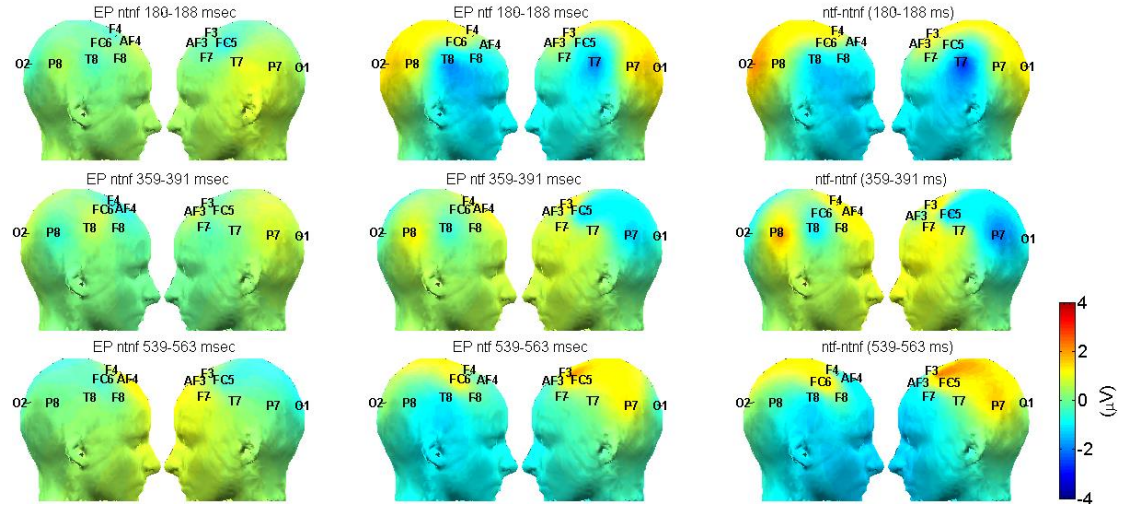

(b)

Figure 36. Flanker-sensitive comparison function at selected electrodes in the EP. (a) difference waves with highlighting significant differences, (b) isopotential maps. (ntf: non-target flanker; ntnf: nontarget non-flanker).

that overcome crowding in these paradigms – effects informative to which interface would better address the crowding and associated fatigue problem. We have shown these biomarkers can both be assessed and the paradigms implemented with ordinary computer equipment using low-cost EEG electronics customizable to measure better EEG signal quality at relatively low-cost [20] – as increases the number of potential users who may benefit from these interface enhancements of their BCI speller.

CHAPTER 7. P300-BASED BRAIN-MOBILE INTERFACE

The comparative study results presented in Chapter 6 emphasize the accuracy and user study advantages of the EP over the ZP and RCP. These results alongside with the EP visual interface nature that increases the distance between adjacent objects and reduces the number of neighbor objects to any another object, makes the EP as a candidate to implement on a mobile simulator with a small screen size. This chapter presents the design, implementation, and evaluation of the mobile BCI. The EP with some changes on its visual interface, mobile EP, to make it more suitable to implement on a device with small screen size is illustrated here.

7.1. Method and Materials

7.1.1. Participants

10 able-bodied human subjects (all male; age 22-35 years; mean: 28 years; s.d.: 3.8) voluntarily participated in this user study. All reported corrected-to-normal or normal vision and being free of neurological diseases. The user study was approved by the Institutional Review Board of North Dakota State University, in accordance with the Declaration of Helsinki. Accordingly, all participants gave informed consent to participate in this study.

7.1.2. Hardware and Data Acquisition

The research edition of the Emotiv EEG wireless headset was used in this study. The EEG signals were recorded by 14 saline electrodes, digitized at 128 Hz, and bandpass filtered 0.16-45 Hz (5^{th} order sinc filter) [24]. The Emotiv EEG deviced was explained in Section 4.1.2.

The digitized and filtered EEG signals then were transmitted via Bluetooth to a Surface Pro 2 device (Windows 8.1 OS; 8 GB RAM; Intel Core i5 processor) through the Emotiv SDK software. The Surface Pro 2 has an HD 10.6 inches (26.924 cm) display. In addition, the EmotivEEG headset toolbox was used to record the EEG

data [36] received from the EEG headset during the BCI speller presentation. The BCI speller system including the speller presentation, data acquisition, preprocessing, and classification was fully developed on MATLAB 7.14.0.739. For the participant's mobility during the experiment, a comfortable and durable wheelchair was used in this study.

7.1.3. Visual Interfaces Design

A Samsung Galaxy S4 smartphone is simulated on the Surface Pro 2 to present the RCP and EP interface, as shown in Figure 37. More specifically, the spellers' interfaces were adapted to fit in the screen of Samsung Galaxy S4 (i.e., 1080 × 1920 pixels, 5.0 inches).

(a) (b)

Figure 37. The Mobile visual interface for the RCP (a) and EP (b).

Both spellers included a matrix of 6-by-6 gray alphanumeric characters. This matrix was displayed with the size of 9.3 × 6.375 cm (interface height (IH) × interface width (IW)) as elaborated in Table 3. Also, there were two text boxes and one *start* command button located below the mobile status bar and above the matrix. One

Table 3. The objects' dimensions and distances between objects for the RCP and EP on a mobile simulator (cm).

Dimensions/Distances	**RCP**	**EP**
Character Height (CH)	0.55	0.55
Character Width (CW)	0.55	0.55
Edge Point Height (EPH)	—	0.55
Edge Point Width (EPW)	—	0.55
Horizontal Inter-character Distance (HICD, HICD1, HICD2)	1.02	0.6, 1.5
Vertical Inter-character Distance (VICD, VICD1, VICD2)	1.55	0.6, 2.49
Horizontal Inter-edge point Distance (HIED)	—	2.1
Vertical Inter-edge point Distance (VIED)	—	3.1
Interface Height (IH)	9.3	9.3
Interface Width (IW)	6.375	6.375

text box was used to input the target characters for the participant to spell, and the second text box displayed the output characters selected by the participant, while the start button was used to run the speller.

In the RCP, as shown in Figure 37(a), the horizontal inter-character distance (*HICD*) between the centres of any two adjacent characters located in the same row is 1.02 cm, and the vertical inter-character distance (*VICD*) is 1.55 cm. Though the matrix in the EP, as illustrated in Figure 37(b), has the same size as the RCP, their distinctions are discussed as follows:

1. A gray square edge point was added to the left (or right) of the odd (or even rows), and below (or above) the odd (or even columns).

2. All characters in rows or columns 2, 4 and 6 were shifted up and left, respectively. Consequently, the horizontal (or vertical distances) between two adjacent rows (or columns) after shifting are increased (refer to *HICD2* and *VICD2* in Table 3).

3. In order to decrease the participant distraction between the target and non-target flash edge points upon opposite side of the matrix, the characters' color was changed to white.

In the RCP, r_i indicates the flashing row with the index i while in the EP, r_i indicates the flashing edge point corresponding to the i^{th} row; and in the RCP, c_i indicates the flashing column with the index i while in the EP, c_i indicates the flashing edge point corresponding to the i^{th} column. The distance between any adjacent row or column edge points is *HIED* or *VIED* (2.1 cm or 3.1cm).

7.1.4. Visual Stimulus Design

A visual flash was used as the visual stimulus in this study. The flash objects in the RCP are rows and columns, while the flash objects are row edge points and column edge points in the EP. For each target character, there were two consecutive stages of random sequences of flashes [84], punctuated by 2 sec of inter-stage interval. In the first stage, depicted in Figure 38 (left panel), there were 72 row flashes in the RCP or row edge point flashes in the EP. In the second stage, there were 72 column flashes in the RCP or column edge point flashes in the EP, as illustrated in Figure 38 (right panel). The stimulus-onset asynchrony (SOA) duration was 120 ms, which consisted of 70 ms as a flash duration and 50 ms as an inter-stimulus interval (ISI). Thus, 19.28 sec was required to select one target character (2 stages * 72 flashes * 0.120 sec SOA + 2 sec inter-stage interval).

In stage 1, the 6 rows or row edge points were each flashed once in a random sequence, as is termed a block. In stage 2, the 6 columns or column edge points were each flashed once in a random sequence, also termed a block. Each stage had 12 blocks. In each block, one flash represented the target object and 5 flashes represented the non-target objects. In other words, in each stage, each target object flashed 12 times (one time per block). Accordingly, 12 out of 72 flashes were considered as the

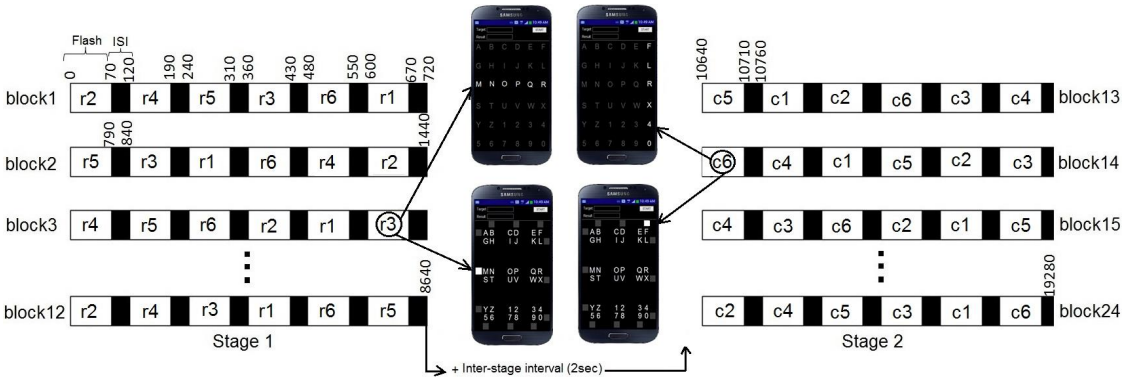

Figure 38. Visual flash and flashing technique for the first stage (left panel), second stage (right panel), and visual flash for flash r_3 from stage 1 and c_6 from stage 2 for both speller (middle panel). The time measurement unit is in ms.

target object flashes (i.e., rare events), and the remaining 60 flashes considered as the non-target flashes (i.e., frequent events).

In order to prevent the double-flash problem caused by flashing the target object twice consecutively [25], a two-stage flashing technique was implemented [84]. For any two consecutive blocks within each stage, the first flashing object in the second block must be different from the last flashing object in the first block. The above technique is formalized as follows.

$$stage1 = \{block_n\}_{n=1}^{12} \tag{7.1}$$

$$block = \{r_i\}_{i=1}^{6} \tag{7.2}$$

$$stage2 = \{block_n\}_{n=13}^{24} \tag{7.3}$$

$$block = \{c_j\}_{j=1}^{6} \tag{7.4}$$

Where in the same stage, $block_n\{flash_1\} \neq block_{n-1}\{flash_6\}$

Where, n is the number of *block* in the first stage ($stage1$) {1, 2, ..., 12} and in the second stage ($stage2$) {13, 14, ..., 24}; r_i is the row or row edge point number, i = {1, 2, 3, 4, 5, 6}; c_i is the column or column edge point number, j = {1, 2, 3, 4, 5, 6}.

7.1.5. Procedure

Each participant completed the two spellers' experiments over two days, one experiment per day, which lasted about 60 minutes. All experiments were counterbalanced to eliminate any confounding effects of order, such that 5 participants started with the RCP and the other 5 participants started with the EP. Each experiment included four successive tasks after the participant signed the consent form, i.e., pre-study questionnaire, offline session, online session, and post-study questionnaire. In the pre-study questionnaire, the participant was asked to rate his fatigue level upon a 10-point Likert item (1: no fatigue to 10: sever fatigue) before using the speller. In the post-study questionnaire, the participant was asked to rate his fatigue level again and to rate his comfort (1: uncomfortable to 10: comfortable) and alertness (1: drowsy to 10: alert) right after using a speller. The participant sat on a comfortable wheelchair and faced the speller with size (9.3×6.375 cm) displayed on the Surface Pro 2 screen at a distance of about 60 cm , as depicted in Figure 39. The Emotiv device was secured to the participant's scalp so as to preclude mechanical electrodes relative to the scalp during the experiment that could contribute to motion artifact. The rigid casing also precluded a contribution of cable sway to motion artifact.

In the RCP, participants were instructed to gaze at the target character in the first and second stages in the RCP. In the EP, participants were instructed to gaze at the target row edge point in the first stage, and then to move their gaze to the target column edge point during the inter-stage interval (2 s) and gaze at it in the second stage. Therefore, the column edge points disappeared during the first stage, whereas the row edge points disappeared during the second stage. In addition, in both spellers, participants were instructed to keep silently counting the number of times the target object flashes. The selected character, which is appended to the output text box, is highlighted with green in the online session.

Figure 39. A snapshot of a participant during the experiment

In the offline session, each participant spelled 6 words and a number (LAP, ROD, BAND, FLAG, DRINK, MINUTE, and 9253) for a total of 29 alphanumeric characters. In the online session, each participant spelled 3 words and a number (FOX, LION, CRAFTS, 40150) for a total of 18 alphanumeric characters. Thus, in both sessions, there were 11 runs for each speller, one run for each word or number, and the participant spelled them character-by-character.

The 18 alphanumeric characters of the online session were selected equally (6 characters) from 3 different areas from the RCP matrix: corner, edge and center areas. More specifically, each corner character was surrounded by 3 adjacent characters, each edge character was surrounded by 5 adjacent characters, and the remaining characters, surrounded by 8 adjacent characters, belonged to the center area of the matrix. This design aimed to investigate how the number of characters surrounding the target character affects the target character selection (i.e., the crowding problem).

While the participant sat on the wheelchair and spelled the target characters in both sessions for both spellers, the experimenter pushed the wheelchair with a speed about 22$\pm$1 meters per minute. The experiment was implemented outside the lab

within normal noise inside a college building during the working hour. Particularly, the experiment was not implemented on a straight path. Thus, the experimenter sometimes turned the wheelchair to the right, left or rotated it smoothly. This wheelchair mobility was continued during each run until the participant spelled the entire word. Then, the experimenter stopped the wheelchair, input another word or number, ran the speller, and moved the wheelchair again.

7.1.6. Preprocessing, Feature Extraction, and Classification

Since the experiments in this study were conducted with the participants' mobility, it was expected that electro-ocular and motion artifacts due to any remaining piezoelectric cable sway and mechanical movement not prevent by rigid cable casing and securing the electrodes to the scalp, alongside noise associated with electromusclar activity [41], alongside the usual artifacts during EEG measurement concerning respiration, cardiac signals, and scalp skin [3, 26, 52], as well as other artificial electrical sources of artifact, such as 60 Hz mains. All these artifacts could contaminate the recordings obscuring the EEG signal. Consequently, a sequence of preprocessing steps was implemented to increase the signal-to-noise ratio (SNR) by de-noising the data. In this study, the EEG signals recorded in stage 1 and in stage 2 were preprocessed, extracted, and classified separately. The first step in the preprocessing used a bandpass filter to pass EEG signals between 0.16 and 45 Hz and downsampled the oversampled data from 2048 Hz to 128 Hz for sake of computational efficiency. The common average referencing technique (CAR) was used to re-reference the data that was physically referenced to the CMS-DRL [17] is a simple, easy, fast, and very necessary technique for multichannel EEG signals to reduce the noise, by $\geq$30%, to detect the small desired signal [64]. Accordingly, the common average referencing technique was applied on the recorded EEG data, where the average across all channels was subtracted from each channel for each data point. The remaining

preprocessing steps, such as winsorizing and normalizing were explained in Section 5.1.6.

The EEG data after preprocessing were extracted based on the time domain feature. However, the EEG data for each single target character were epoched to 600 ms from each flash onset. Each epoch with 600 ms size of data was called a segment, and each segment contained the ERP produced in consequence of neurocognitive processes corresponding to one visual flash. Each segment contained data recorded by 14 channels in 77 time points (0.600 s * 128 sample/s). For each target character with 144 flashes, there were 144 segments; one segment corresponded to one flash. Specifically, 72 row or row edge point segments and 72 column or column edge point segments.

Now, the classification can realize the new format of segment features. The Bayesian Linear Discriminant Analysis (BLDA) was used in this study to identify the target character. The classification detail process was explained in Section 5.1.6.

7.2. Results

7.2.1. Online Character-based Classification Accuracy

In the online session, 180 characters (18 characters * 10 participants) were selected for each speller. As depicted in Figure 40, the online classification accuracy was improved with the EP, mean 89.44 ± s.e.m 2.1%, relative to RCP, 80.55±2.65%. A paired t-test was used for the inferential statistical analysis and confirmed that the accuracy for the EP was significantly higher than the RCP, $t(9) = 3.205$, $p = 0.011$, $\eta^2 = 0.533$ (8/10 showed the effect).

7.2.2. Flash Object-based Analysis of Adjacent Errors

Further analyses were applied to the incorrectly selected characters by investigating the flash objects. The flash object may be the row and column in the RCP or row edge point and column edge point in the EP. These analyses aimed to determine

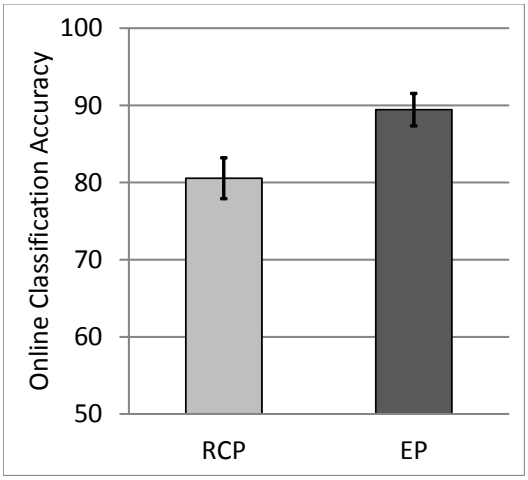

Figure 40. Mean percentage classification accuracy as a function of interface (error bars denote standard error); N=10.

if the online performance improvement with the EP over RCP were caused by the adjacent distance between flash objects. Hypothetically, if the number of adjacent errors with the RCP is significantly higher than the number of adjacent errors in the EP, then the adjacent distance between the flashed object played a vital role that affect the online performance.

As shown in Figure 41, the 180 online selected characters, for each speller, were summarized within a confusion matrix of errors, denoted by m. The rows and column indices for m were from -5 to 5. If the online character was correctly selected, then the number of characters selected correctly, located in the center cell $m(0,0)$ and highlighted in gray, is incremented by 1, where the row index '0' and column index '0' represent the target row and target column, respectively. All cells in m except $m(0,0)$ represent the error locations in the speller, and the total number of these cell values is the total number of errors. In general, the cell position in m for any selected character from the speller was identified by m(selected row - target row, selected column - target column). For example, if the target character 'L', which is located on the row 2 and column 6 in a speller interface, was selected correctly, then the value

in cell $m(0,0)$ is incremented by 1; otherwise, if the target character 'L' was selected incorrectly by 'F', which is located on row 1 and column 6, then the value in cell $m(1\text{-}2, 6\text{-}6) = m(\text{-}1, 0)$ is incremented by 1.

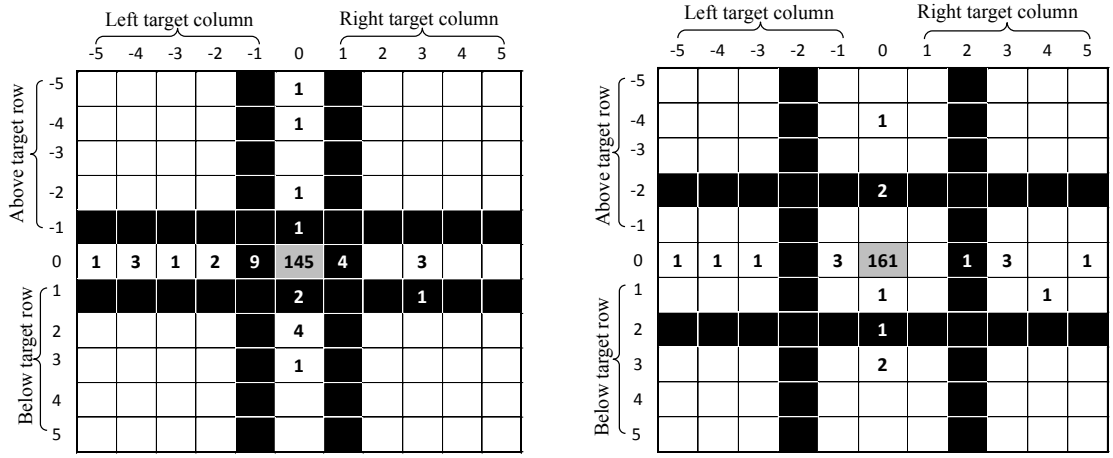

Figure 41. The error confusion matrix (m) of all subjects for 180 selected characters in the online session for the RCP (a) and EP (b); the gray center cell denoting the target; black cells denoting adjacent flashed object errors, where a neighboring flash was erroneously detected as denoting the row or column of the target.

Parenthetically, the horizontal (row) and vertical (column) adjacent error selected characters were located in the highlighted black cells, as depicted in Figure 41. For both spellers, as illustrated in Figure 41(a) and Figure 41(b), the horizontal adjacent flash object(s) for any target flash object was located in row '-1' and row '1' in m for the RCP, or row '-2' and row '2' for the EP. The vertical adjacent flash object(s) for any target flash object was located in column '-1' and column '1' in m for the RCP, or column '-2' and column '2' for the EP.

The numbers of the horizontal and vertical adjacent errors in the RCP were larger than in the EP. Thus, the influence of the adjacent problem was reduced by increasing the distance between the adjacent flash objects with the EP. Of a total of 35 errors for the RCP, there were 4 horizontal adjacent errors (11.4%) and 13

vertical adjacent errors (37.4%). Of a total of 19 errors for the EP, there were 3 horizontal adjacent errors (15.79%) and 1 vertical adjacent errors (5.26%). A paired samples t-test showed that the mean±s.e.m of horizontal adjacent errors was non-significant between the RCP (mean 0.4±s.e.m 0.306) and EP (0.3±0.153). In contrast, the mean±s.e.m of vertical adjacent errors was significantly higher for the RCP (1.3±0.367) relative to the EP (0.1±0.1), $t(9) = -3.674$, $p = 0.005$, $\eta^2 = 0.6$ (7/10 showed the effect).

7.2.3. Errors Analysis for the RCP

Each online character was located on the center, edge, or corner of the speller matrix and surrounded by 3, 5, 8 and characters, respectively. In this investigation, 6 characters were selected from each speller matrix area (6 characters per area * 3 areas = 18 online characters) and tested by 10 participants (6 * 10 = 60 test characters per area from all participants).

In the RCP, of a total of 60 selected characters from each area, there were 14 selected error characters (23.33%) for the center area, 11 selected error characters (18.33%) for the edge area, and 10 selected error characters (16.67%) for the corner area. A one-way ANOVA upon error selection from the different three matrix areas not revealed any significant between these matrix areas.

7.2.4. User Experience

The pre- and post-study questionnaire data measured the subjective ratings of fatigue, comfort, and alertness in both paradigms. The subjective rating range was upon 10-point Likert item 1 to 10, and the difference between the fatigue rating before and after the experiment was between 0 to 9, where 0 and 9 indicated the best and worst level of fatigue, respectively, caused by use of the speller. Conversely, 10 indicated the ideal for comfort and alertness. As shown in Figure 42(a), the mean±s.m.e fatigue level was reduced with the EP, 1.8±0.44, relative to RCP, 4±0.47.

Also, participants were felt more comfortable after using the EP, 8.6±0.27, relative to the RCP, 5.7±0.7, as well as more alert during spelling from the EP, 8.7±0.34, relative to the RCP, 6.1±0.67, as shown in Figure 42(b).

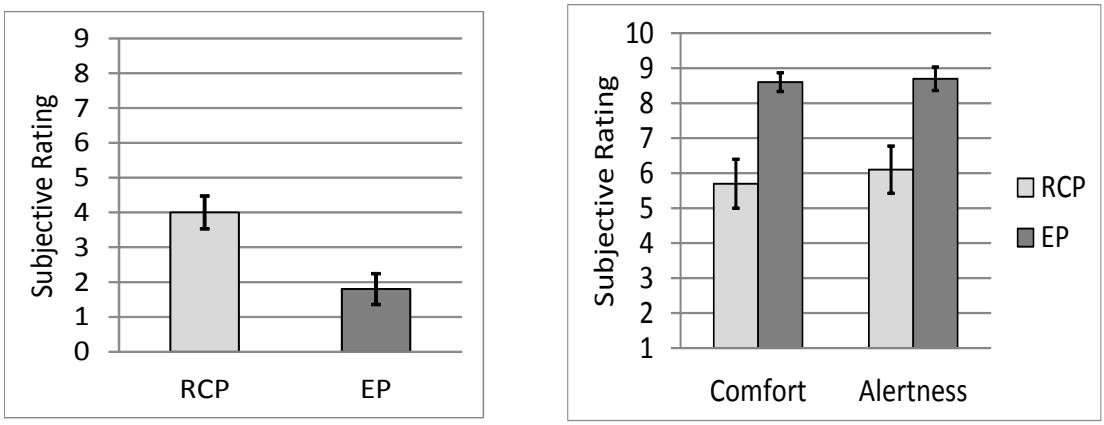

(a) (b)

Figure 42. Subjective rating for all participants (N=10). (a) Mean of the fatigue rating difference before and after the experiment (0:9). (0: lowest level of fatigue, 9: highest level of fatigue). (b) Mean of the comfort, and alertness rating (1:10). (1: lowest level of comfort and alertness, 10: highest level of comfort and alertness).

These tendencies shown in Figure 42 were broadly confirmed by inferential statistical analyses: Paired t-tests comparing EP and RCP revealed a significant effect of the interface upon fatigue, $t(9) = 3.236$, $p = 0.01$, $\eta^2 = 0.54$ (8/10 showed the effect), upon comfort, $t(9) = -3.585$, $p = 0.006$, $\eta^2 = 0.59$ (9/10 showed the effect), and upon alertness, $t(9) = -3.284$, $p = 0.009$, $\eta^2 = 0.54$ (8/10 showed the effect).

7.3. Discussion

The results of this study were consistent with the finding of Chapter 5 and 6 results, and confirmed that the EP significantly improved the online classification accuracy and user experience over the RCP during both the sitting or mobility situations, as well as with small or large speller interface. In addition, the EP caused significantly less fatigue, more comfort, and more alertness relative to the RCP.

In general, the EP reduced the effect of adjacent, crowding, and fatigue problems, altogether, by adding a flash edge point to each row and column, shifting every second row or column up and left, respectively, and changing the flashing technique and its illumination size.

In the RCP, relatively, a large number of errors were horizontal or vertical adjacent errors [27, 72, 90]. In addition, the number of adjacent errors was significantly higher for the RCP than EP. Some participants' spontaneously volunteers subjective qualitative reports of a perceived interference between adjacent flash object while moving, as was particularly apparent when using the RCP rather than the EP. The further RCP errors analysis showed that the number of errors increased from the corner area to edge area to center area. These differences of errors upon the matrix areas were not significant. Increasing the number of participants in this study may increase the differences between numbers of errors upon matrix areas.

In the EP, the white alphanumeric characters reduced the crowding problem by increasing a spatial separator between edge points upon opposite sides of the matrix. Furthermore, the white characters reduced the fatigue problem by decreasing the participant distraction between the target and non-target (i.e., distractors) flashes [29, 1].

If some mobile applications required displaying larger than 6-by-6 matrix of objects, then the EP is the more suitable interface design choice rather than RCP. In more details, the EP can increase the matrix dimension size, i.e., number of objects, and keep the number of flash objects surrounding any target flash to 1 or 2, but the distance between the two adjacent flash row edge points or column edge points is reduced as in the RCP.

CHAPTER 8. CONCLUSION AND FUTURE WORK

The motivation of this dissertation has been to improve the performance and user experience with P300-based BCI. Accordingly, this dissertation has presented new P300 BCIs to reduce the aforementioned challenges of the most popular P300 BCI, RCP. In particular, two P300 BCIs were developed – ZP and EP. In the ZP, every second row of the objects matrix shifted to the right by $d/2$ cm, where d cm is the distance between two adjacent characters located on the same row. In the EP, a flash grey edge point added to the left side of every odd row, right side of each even row, below every odd column, and above each even column.

In this work, four user studies were conducted to evaluate the performance and user experience of the new proposed P300 BCIs and compare them with each other and with the classical RCP. The first user study was conducted on the desktop to evaluate the ZP and compare it with the RCP. A user study upon neurologically normal individuals revealed significant improvements in online classification performance and user experience with the ZP. Improvements of online classification performance with ZP showed that ZP offered a solution to the crowding problem and adjacency problem, while the potentially related improvements in user experience showed that ZP also provided an effective approach to the fatigue problem.

In the second user study, the investigation has shown that the previously unexplored modifications of the P300-based BCI by the EP interface have exhibited advantages over the classical RCP on the desktop. The EP demonstrated significant improvements in the online classification performance and user experience found with the RCP, attributable to a reduced influence of the crowding and adjacency problems, in turn, causing less fatigue and yielding significantly improved levels of alertness and comfort. The key principles of the EP were to reduce the influence of the adjacency problem by increasing the distance between adjacent flashed objects and to reduce

the influence of the crowding problem by decreasing the number of similar flashed objects surrounding any object.

In the third user study, all P300 BCIs (RCP, ZP, and EP) were evaluated on the desktop. The results showed that the speller online classification performance and the user experience were significantly improved from the RCP to ZP to EP. The results indicated that the EP offered better solutions to the adjacent and crowding problems relative to the ZP. Further, this investigation has shown that the EP overcomes the limitations of the RCP and ZP as a candidate class of interface for such mobile BCIs.

In the fourth study, the P300 BCIs, specifically the EP and RCP, were moved to the mobile platform and evaluated during the user's mobility using a wheelchair in a normal noisy environment. This study allows disabled users to benefit the fast development in the mobile computing. This study confirmed that the EP is suitable for use upon a mobile device. The results of this investigation also revealed that the online classification accuracy and user experience of the EP significantly improved over the RCP.

In sum, the conclusion of this dissertation demonstrates that the large distance between adjacent flash objects and the fewer objects subject to visuospatial crowding increased the performance accuracy, as well as reducing the number of errors, and attenuating the influence of the user fatigue problem during the use of the interface. Although the mobile EP speller implemented on a mobile phone simulator offers a suitable interface for small screen size, at a future time prior to valorization of this research, it would be recommended to evaluate a prototype speller implemented on an extant mobile phone.

In the future, this work can be expanded to implement the mobile EP on the actual mobile phone and address most challenges that come up from the limited, though ever-evolving specification of extant mobile phones, specifically the processor

and memory. These challenges can be addressed by: reducing the amount of EEG data, using advance filtering process, using a medical-grade wireless EEG device with the optimal positioning of electrodes, designing a light and accurate machine learning algorithm that operates at high speed upon a mobile phone, and programming in C++ or Java programming rather than MATLAB. C++ and Java are OS platform-independent and running under Windows and Android environments, in a manner that could increase speed of the speller presentation, preprocessing, and classification. Furthermore, the mobile EP can be used to implement a set of mobile phone applications, which help paralyzed people with minimal voluntary muscular control to utilize the advantages of mobile computing and features.

Another future direction is to utilize the datasets collected from each conducted study for further analysis, such as channel selection and decimation (i.e., downsampling to less than 128 Hz), in order to reduce the dimension vectors for each segment (i.e., classification features). This reduction can accelerate the data processing, particularly in a smartphone. In addition, these datasets can be further investigated with the aim of examining the effect of different bandpass filtering boundaries on the classification accuracy.

REFERENCES

[1] Brendan Z Allison and Jaime A Pineda, *Erps evoked by different matrix sizes: implications for a brain computer interface (bci) system*, IEEE T Neur Sys Reh. **11** (2003), no. 2, 110–113.

[2] Fabio Aloise, Francesca Schettini, Pietro Aricò, Serenella Salinari, Fabio Babiloni, and Febo Cincotti, *A comparison of classification techniques for a gaze-independent p300-based brain–computer interface*, Journal of neural engineering **9** (2012), no. 4, 045012.

[3] Peter Anderer, Stephen Roberts, A Schlögl, Georg Gruber, G Klösch, Werner Herrmann, Peter Rappelsberger, Oliver Filz, Manel J Barbanoj, Georg Dorffner, et al., *Artifact processing in computerized analysis of sleep eeg–a review*, Neuropsychobiology **40** (1999), no. 3, 150–157.

[4] Erol Başar, Canan Başar-Eroglu, Sirel Karakaş, and Martin Schürmann, *Gamma, alpha, delta, and theta oscillations govern cognitive processes*, International Journal of Psychophysiology **39** (2001), no. 2, 241–248.

[5] Jean-Dominique Bauby, *The diving bell and the butterfly*, Random House LLC, 2008.

[6] Andrei Belitski, Jason Farquhar, and Peter Desain, *P300 audio-visual speller*, Journal of neural engineering **8** (2011), no. 2, 025022.

[7] Yoav Benjamini and Daniel Yekutieli, *The control of the false discovery rate in multiple testing under dependency*, Annals of statistics (2001), 1165–1188.

[8] Hans Berger, *Über das elektrenkephalogramm des menschen*, European Archives of Psychiatry and Clinical Neuroscience **87** (1929), no. 1, 527–570.

[9] Niels Birbaumer, Nimr Ghanayim, Thilo Hinterberger, Iver Iversen, Boris Kotchoubey, Andrea Kübler, Juri Perelmouter, Edward Taub, and Herta Flor, *A spelling device for the paralysed*, Nature **398** (1999), no. 6725, 297–298.

[10] Benjamin Blankertz, Matthias Krauledat, Guido Dornhege, John Williamson, Roderick Murray-Smith, and Klaus-Robert Müller, *A note on brain actuated spelling with the berlin brain-computer interface*, Universal Access in Human-Computer Interaction. Ambient Interaction, Springer, 2007, pp. 759–768.

[11] Christoph Bledowski, David Prvulovic, Karsten Hoechstetter, Michael Scherg, Michael Wibral, Rainer Goebel, and David EJ Linden, *Localizing p300 generators in visual target and distractor processing: a combined event-related potential and functional magnetic resonance imaging study*, The Journal of neuroscience **24** (2004), no. 42, 9353–9360.

[12] Herman Bouma, *Interaction effects in parafoveal letter recognition*, Nature **226** (1970), 177–178.

[13] Anne-Marie Brouwer and Jan BF Van Erp, *A tactile p300 brain-computer interface*, Front. Neurosci. **4**.

[14] Peter Brunner, S Joshi, Samuel Briskin, Jonathan R Wolpaw, Horst Bischof, and Gerwin Schalk, *Does the 'p300' speller depend on eye gaze?*, Journal of neural engineering **7** (2010), no. 5, 056013.

[15] Paul F Bulakowski, Robert B Post, and David Whitney, *Visuomotor crowding: the resolution of grasping in cluttered scenes*, Front Behav Neurosci. **3** (2009), no. 49.

[16] Andrew Campbell, Tanzeem Choudhury, Shaohan Hu, Hong Lu, Matthew K Mukerjee, Mashfiqui Rabbi, and Rajeev DS Raizada, *Neurophone: brain-mobile phone interface using a wireless eeg headset*, Proceedings of the second ACM SIGCOMM workshop on Networking, systems, and applications on mobile handhelds, ACM, 2010, pp. 3–8.

[17] Tom Campbell, Jess R Kerlin, Christopher W Bishop, and Lee M Miller, *Methods to eliminate stimulus transduction artifact from insert earphones during electroencephalography*, Ear and hearing **33** (2012), no. 1, 144.

[18] Jacob Cohen, *Statistical power analysis for the behavioral sciences*, Psychology Press, 1988.

[19] Max Coltheart, *The mrc psycholinguistic database*, Q J Exp Psychol. **33** (1981), no. 4, 497–505.

[20] Stefan Debener, Falk Minow, Reiner Emkes, Katharina Gandras, and Maarten Vos, *How about taking a low-cost, small, and wireless eeg for a walk?*, Psychophysiology **49** (2012), no. 11, 1617–1621.

[21] Wm H Dobelle, *Artificial vision for the blind by connecting a television camera to the visual cortex*, ASAIO journal **46** (2000), no. 1, 3–9.

[22] Emanuel Donchin, *Surprise! surprise?*, Psychophysiology **18** (1981), no. 5, 493–513.

[23] Denise Dudzinski, *The diving bell meets the butterfly: Identity lost andremembered*, Theoretical medicine and bioethics **22** (2001), no. 1, 33–46.

[24] EmotivSystem, *Emotiv: brain–computer interface technology*, `http://www.emotiv.com` [Online; accessed May 23, 2013].

[25] Lawrence Ashley Farwell and Emanuel Donchin, *Talking off the top of your head: toward a mental prosthesis utilizing event-related brain potentials*, Electroen Clin Neuro **70** (1988), no. 6, 510–523.

[26] Mehrdad Fatourechi, Ali Bashashati, Rabab K Ward, and Gary E Birch, *Emg and eog artifacts in brain computer interface systems: A survey*, J Clin Neurophysiol. **118** (2007), no. 3, 480–494.

[27] Reza Fazel-Rezai, *Human error in p300 speller paradigm for brain-computer interface*, Engineering in Medicine and Biology Society, 2007. EMBS 2007. 29th Annual International Conference of the IEEE, IEEE, 2007, pp. 2516–2519.

[28] Reza Fazel-Rezai and Kamyar Abhari, *A region-based p300 speller for brain-computer interface*, Can J Elect Comput E. **34** (2009), no. 3, 81–85.

[29] Fatima M Felisberti, Joshua A Solomon, and Michael J Morgan, *The role of target salience in crowding*, PERCEPTION-LONDON- **34** (2005), no. 7, 823.

[30] Chengzhi Feng, Yi Jiang, and Sheng He, *Horizontal and vertical asymmetry in visual spatial crowding effects*, J Vision. **7** (2007), no. 2, 13.

[31] Alessandro L. Stamatto Ferreira, Leonardo Cunha de Miranda, Erica E. Cunha de Miranda, and Sarah Gomes Sakamoto, *A survey of interactive systems based on brain-computer interfaces*, SBC Journal on 3D Interactive Systems **4** (2013), no. 1, 3–13 ISSN: 2236–3297.

[32] Jonathan R Folstein and Cyma Van Petten, *Influence of cognitive control and mismatch on the n2 component of the erp: a review*, Psychophysiology **45** (2008), no. 1, 152–170.

[33] Stefan Frenzel, Elke Neubert, and Christoph Bandt, *Two communication lines in a 3 × 3 matrix speller*, Journal of neural engineering **8** (2011), no. 3, 036021.

[34] Gerald Frye, Christopher Hauser, George Townsend, and EW Sellers, *Suppressing flashes of items surrounding targets during calibration of a p300-based brain–computer interface improves performance*, Journal of neural engineering **8** (2011), no. 2, 025024.

[35] Adrian Furdea, Sebastian Halder, Dean Krusienski, D Bross, Femke Nijboer, Niels Birbaumer, and Andrea Kübler, *An auditory oddball (p300) spelling system for brain-computer interfaces*, Psychophysiology **46** (2009), no. 3, 617–625.

[36] Paul Gavin, *EmotivEEG headset toolbox*, Matlab Central File Exchange, `http://www.mathworks.com/matlabcentral/fileexchange/36111-emotiveeg-headset-toolbox` [Online; accessed May 23, 2013].

[37] Ken J Gilhooly and Robert H Logie, *Age-of-acquisition, imagery, concreteness, familiarity, and ambiguity measures for 1,944 words*, Behav Res Meth Instr. **12** (1980), no. 4, 395–427.

[38] David M Groppe, Thomas P Urbach, and Marta Kutas, *Mass univariate analysis of event-related brain potentials/fields i: A critical tutorial review*, Psychophysiology **48** (2011), no. 12, 1711–1725.

[39] Christoph Guger, Shahab Daban, Eric Sellers, Clemens Holzner, Gunther Krausz, Roberta Carabalona, Furio Gramatica, and Guenter Edlinger, *How many people are able to control a p300-based brain–computer interface (bci)?*, Neurosci Lett. **462** (2009), no. 1, 94–98.

[40] Christoph Guger, Clemens Holzner, Christoph Groenegress, Günter Edlinger, and Mel Slater, *Brain computer interface for virtual reality control.*, ESANN, 2009.

[41] Joseph T Gwin, Klaus Gramann, Scott Makeig, and Daniel P Ferris, *Removal of movement artifact from high-density eeg recorded during walking and running.*, Journal of neurophysiology **103** (2010), no. 6, 3526–3534.

[42] Matti Hämäläinen, Riitta Hari, Risto J Ilmoniemi, Jukka Knuutila, and Olli V Lounasmaa, *Magnetoencephalographytheory, instrumentation, and applications to noninvasive studies of the working human brain*, Reviews of modern Physics **65** (1993), no. 2, 413.

[43] Stephen W Hawking, *A brief history of time. book*, 1988.

[44] Leigh R Hochberg, Mijail D Serruya, Gerhard M Friehs, Jon A Mukand, Maryam Saleh, Abraham H Caplan, Almut Branner, David Chen, Richard D Penn, and John P Donoghue, *Neuronal ensemble control of prosthetic devices by a human with tetraplegia*, Nature **442** (2006), no. 7099, 164–171.

[45] Ulrich Hoffmann, *Bayesian machine learning applied in a brain-computer interface for disabled users*, Ph.D. thesis, ÉCOLE POLYTECHNIQUE FÉDÉRALE DE LAUSANNE, 2007.

[46] Ulrich Hoffmann, Jean-Marc Vesin, Touradj Ebrahimi, and Karin Diserens, *An efficient p300-based brain–computer interface for disabled subjects*, J Neurosci Meth. **167** (2008), no. 1, 115–125.

[47] Shiro Ikegami, Kouji Takano, Naokatsu Saeki, and Kenji Kansaku, *Operation of a p300-based brain–computer interface by individuals with cervical spinal cord injury*, Clinical Neurophysiology **122** (2011), no. 5, 991–996.

[48] Iñaki Iturrate, Javier Mauricio Antelis, Andrea Kübler, and Javier Minguez, *A noninvasive brain-actuated wheelchair based on a p300 neurophysiological protocol and automated navigation*, IEEE T Robot. **25** (2009), no. 3, 614–627.

[49] Jing Jin, Brendan Z Allison, Eric W Sellers, Clemens Brunner, Petar Horki, Xingyu Wang, and Christa Neuper, *An adaptive p300-based control system*, Journal of neural engineering **8** (2011), no. 3, 036006.

[50] Jing Jin, Brendan Z Allison, Eric W Sellers, Clemens Brunner, Petar Horki, Xingyu Wang, and Christa Neuper, *Optimized stimulus presentation patterns for an event-related potential eeg-based brain–computer interface*, Medical & biological engineering & computing **49** (2011), no. 2, 181–191.

[51] Jing Jin, Brendan Z Allison, Xingyu Wang, and Christa Neuper, *A combined brain–computer interface based on p300 potentials and motion-onset visual evoked potentials*, Journal of neuroscience methods **205** (2012), no. 2, 265–276.

[52] Emily S Kappenman and Steven J Luck, *The effects of electrode impedance on data quality and statistical significance in erp recordings*, Psychophysiology **47** (2010), no. 5, 888–904.

[53] Tobias Kaufmann, Stefan Schulz, Claudia Grünzinger, and Andrea Kübler, *Flashing characters with famous faces improves erp-based brain–computer interface performance*, Journal of neural engineering **8** (2011), no. 5, 056016.

[54] Albert Kok, *On the utility of p3 amplitude as a measure of processing capacity*, Psychophysiology **38** (2001), no. 3, 557–577.

[55] Steven Kotler, *Vision quest*, Wired Magazine **10** (2002).

[56] Dean J Krusienski, Eric W Sellers, François Cabestaing, Sabri Bayoudh, Dennis J McFarland, Theresa M Vaughan, and Jonathan R Wolpaw, *A comparison of classification techniques for the p300 speller*, J Neural Eng. **3** (2006), no. 4, 299.

[57] Edmund C Lalor, Simon P Kelly, Ciarán Finucane, Robert Burke, Ray Smith, Richard B Reilly, and Gary Mcdarby, *Steady-state vep-based brain-computer interface control in an immersive 3d gaming environment*, EURASIP journal on applied signal processing **2005** (2005), 3156–3164.

[58] Robert Leeb, Doron Friedman, Gernot R Müller-Putz, Reinhold Scherer, Mel Slater, and Gert Pfurtscheller, *Self-paced (asynchronous) bci control of a wheelchair in virtual environments: a case study with a tetraplegic*, Computational intelligence and neuroscience **2007** (2007).

[59] Janne Lehtonen, *EEG-based brain computer interfaces*, Master's thesis, Helsinky University Of Technology, Department of Electrical and Communication Engineering, 2002.

[60] Xu Lei, Ping Yang, and Dezhong Yao, *An empirical bayesian framework for brain–computer interfaces*, Neural Systems and Rehabilitation Engineering, IEEE Transactions on **17** (2009), no. 6, 521–529.

[61] Jessica Lu, William Speier, Xiao Hu, and Nader Pouratian, *The effects of stimulus timing features on p300 speller performance*, Clinical Neurophysiology **124** (2013), no. 2, 306–314.

[62] Steven J Luck, *Ten simple rules for designing erp experiments*, Event-related potentials: A methods handbook **262083337** (2005).

[63] Steven J Luck and Emily S Kappenman, *The oxford handbook of event-related potential components*, Oxford university press, 2011.

[64] Kip A Ludwig, Rachel M Miriani, Nicholas B Langhals, Michael D Joseph, David J Anderson, and Daryl R Kipke, *Using a common average reference to improve cortical neuron recordings from microelectrode arrays*, Journal of neurophysiology **101** (2009), no. 3, 1679.

[65] David JC MacKay, *Bayesian interpolation*, Neural computation **4** (1992), no. 3, 415–447.

[66] Nikolay V Manyakov, Nikolay Chumerin, Adrien Combaz, and Marc M Van Hulle, *Comparison of classification methods for p300 brain-computer interface on disabled subjects*, Computational intelligence and neuroscience **2011** (2011), 2.

[67] Axel Mecklinger, Burkhard Maess, Bertram Odashing same author nametz, Erdmut Pfeifer, Douglas Cheyne, and Harold Weinberg, *A meg analysis of the p300 in visual discrimination tasks*, Electroencephalography and Clinical Neurophysiology/Evoked Potentials Section **108** (1998), no. 1, 45–56.

[68] Peter Meinicke, Matthias Kaper, Florian Hoppe, Manfred Heumann, and Helge Ritter, *Improving transfer rates in brain computer interfacing: a case study*, Adv Neur In (NIPS), 2002, pp. 1107–1114.

[69] Emily Muglerab, Michael Benschc, Sebastian Haldera, Wolfgang Rosenstielc, Martin Bogdancd, Niels Birbaumerae, and Andrea Kübler, *Control of an internet browser using the p300 event-related potential*, Int J Bioelectromagn. **10** (2008), no. 1, 56–63.

[70] United Nation, *Deputy un chief calls for urgent action to tackle global sanitation crisis*, `http://www.un.org/apps/news/story.asp//story.asp?NewsID=44452&Cr=sanitation&Cr1=#.UykerfldWyQ` [Online; accessed March 18, 2014].

[71] Luis Fernando Nicolas-Alonso and Jaime Gomez-Gil, *Brain computer interfaces, a review*, Sensors **12** (2012), no. 2, 1211–1279.

[72] Qasem Obeidat, Tom Campbell, and Jun Kong, *The zigzag paradigm: a new p300-based brain computer interface*, Proceedings of the 15th ACM on International conference on multimodal interaction, ACM, 2013, pp. 205–212.

[73] Gabriel Pires, Urbano Nunes, and Miguel Castelo-Branco, *GIBS block speller: toward a gaze-independent p300-based BCI*, Engineering in Medicine and Biology Society, EMBC, 2011 Annual International Conference of the IEEE, IEEE, 2011, pp. 6360–6364.

[74] Gabriel Pires, Urbano Nunes, and Miguel Castelo-Branco, *Comparison of a row-column speller vs. a novel lateral single-character speller: Assessment of bci for severe motor disabled patients*, Clinical Neurophysiology **123** (2012), no. 6, 1168–1181.

[75] John Polich, *Theoretical overview of p3a and p3b*, Detection of Change, Springer, 2003, pp. 83–98.

[76] John Polich, *Updating p300: an integrative theory of p3a and p3b*, Clinical neurophysiology **118** (2007), no. 10, 2128–2148.

[77] C-C Postelnicu and Doru Talaba, *P300-based brain-neuronal computer interaction for spelling applications*, Biomedical Engineering, IEEE Transactions on **60** (2013), no. 2, 534–543.

[78] Brice Rebsamen, Etienne Burdet, Cuntai Guan, Haihong Zhang, Chee Leong Teo, Qiang Zeng, Marcelo Ang, and Christian Laugier, *A brain-controlled wheelchair based on p300 and path guidance*, Biomedical Robotics and Biomechatronics, 2006. BioRob 2006. The First IEEE/RAS-EMBS International Conference on, IEEE, 2006, pp. 1101–1106.

[79] Robert L Rogers, Stephen B Baumann, Andrew C Papanicolaou, Thomas W Bourbon, Sudar Alagarsamy, and Howard M Eisenberg, *Localization of the p3 sources using magnetoencephalography and magnetic resonance imaging*, Electroencephalography and clinical Neurophysiology **79** (1991), no. 4, 308–321.

[80] David B Ryan, Gerald Frye, George Townsend, DR Berry, S Mesa-G, Nathan A Gates, and Eric W Sellers, *Predictive spelling with a p300-based brain–computer interface: Increasing the rate of communication*, Intl. Journal of Human–Computer Interaction **27** (2010), no. 1, 69–84.

[81] Mathew Salvaris and Francisco Sepulveda, *Visual modifications on the p300 speller bci paradigm*, J Neural Eng. **6** (2009), no. 4, 046011.

[82] Saeid Sanei and Jonathon A Chambers, *Eeg signal processing*, John Wiley & Sons, 2008.

[83] Eric W Sellers, Dean J Krusienski, Dennis J McFarland, Theresa M Vaughan, and Jonathan R Wolpaw, *A p300 event-related potential brain–computer interface (bci): the effects of matrix size and inter stimulus interval on performance*, Biol Psychol. **73** (2006), no. 3, 242–252.

[84] Hilit Serby, Elad Yom-Tov, and Gideon F Inbar, *An improved p300-based brain-computer interface*, IEEE T Neur Sys Reh. **13** (2005), no. 1, 89–98.

[85] Frank Sharbrough, GE Chatrian, Ronald Lesser, Hans Lüders, Marc Nuwer, and Terence Picton, *American electroencephalographic society guidelines for standard electrode position nomenclature*, J. Clin. Neurophysiol. **8** (1991), no. 2, 200–202.

[86] Zachary Simmons, BA Bremer, RA Robbins, SM Walsh, and S Fischer, *Quality of life in ALS depends on factors other than strength and physical function*, Neurology **55** (2000), no. 3, 388–392.

[87] Samuel Sutton, Margery Braren, Joseph Zubin, and ER John, *Evoked-potential correlates of stimulus uncertainty*, Science **150** (1965), no. 3700, 1187–1188.

[88] Kouji Takano, Tomoaki Komatsu, Naoki Hata, Yasoichi Nakajima, and Kenji Kansaku, *Visual stimuli for the p300 brain–computer interface: a comparison of white/gray and green/blue flicker matrices*, Clinical neurophysiology **120** (2009), no. 8, 1562–1566.

[89] Marta Teixeira, Miguel CASTELO-BRANCO, SM NASCIMENTO, and VMN ALMEIDA, *The p300 signal is monotonically modulated by target saliency level irrespective of the visual feature domain*, Acta Ophthalmologica **88** (2010), no. s246, 0–0.

[90] George Townsend, Brandon LaPallo, Chadwick Boulay, Dean Krusienski, Gerald Frye, Christopher Hauser, NE Schwartz, Theresa Vaughan, Jonathan R Wolpaw, and Eric Sellers, *A novel p300-based brain–computer interface stimulus presentation paradigm: moving beyond rows and columns*, J Clin Neurophysiol. **121** (2010), no. 7, 1109–1120.

[91] George Townsend, Jessica Shanahan, David B Ryan, and Eric W Sellers, *A general p300 brain–computer interface presentation paradigm based on performance guided constraints*, Neuroscience letters **531** (2012), no. 2, 63–68.

[92] Matthias S Treder and Benjamin Blankertz, *(c) overt attention and visual speller design in an erp-based brain-computer interface*, Behav Brain Funct. **6** (2010), no. 1, 28.

[93] Matthias Sebastian Treder, Nico Maurice Schmidt, and Benjamin Blankertz, *Gaze-independent brain–computer interfaces based on covert attention and feature attention*, Journal of neural engineering **8** (2011), no. 6, 066003.

[94] David Whitney and Dennis M Levi, *Visual crowding: A fundamental limit on conscious perception and object recognition*, Trends Cogn Sci. **15** (2011), no. 4, 160–168.

[95] Jonathan R Wolpaw, Niels Birbaumer, William J Heetderks, Dennis J McFarland, P Hunter Peckham, Gerwin Schalk, Emanuel Donchin, Louis A Quatrano, Charles J Robinson, Theresa M Vaughan, et al., *Brain-computer interface technology: a review of the first international meeting*, IEEE transactions on rehabilitation engineering **8** (2000), no. 2, 164–173.

[96] Jonathan R Wolpaw, Niels Birbaumer, Dennis J McFarland, Gert Pfurtscheller, and Theresa M Vaughan, *Brain–computer interfaces for communication and control*, J Clin Neurophysiol. **113** (2002), no. 6, 767–791.

[97] Jonathan R Wolpaw and Elizabeth Winter Wolpaw, *Brain-computer interfaces: principles and practice*, Oxford University Press, 2012.

[98] Y Xu and Y Nakajima, *A two-level predictive event-related potential-based brain-computer interface.*, IEEE transactions on bio-medical engineering **60** (2013), no. 10, 2839.

[99] Tianyou Yu, Yuanqing Li, Jinyi Long, and Zhenghui Gu, *Surfing the internet with a bci mouse*, Journal of neural engineering **9** (2012), no. 3, 036012.